Arab J Geosci (2016) 9: 70
DOI 10.1007/s12517-015-2056-4

ORIGINAL PAPER

Depositional environment, diagenesis, and geochemistry of Devonian Bahram formation carbonates, Eastern Iran

Mahdi Hoseinabadi[1] · Asadollah Mahboubi[2] · Gholamreza Mirab Shabestari[3] · Ahmad Motamed[4]

Received: 28 October 2014 / Accepted: 10 September 2015 / Published online: 17 December 2015

Abstract The Middle-Upper Devonian Bahram Formation carbonates in eastern Iran were investigated in three stratigraphic sections including Cheshmeh Shir (NE Tabas), Kamar Kuh (S Kashmar), and Hozedorah (E Tabas), in order to define their depositional environment, diagenesis, and geochemistry of major and minor elements. Petrographic and microfacies pattern studies led to the recognition of five microfacies groups including shore face, tidal flat, lagoonal, shoal and open-marine facies. Evidences such as absence of calciturbidite deposits, reefal facies, slumping and sliding facies, gradual facies changes, absence of the special grains of carbonate shelf such as cortoid, oncoid, pisoid, and aggregate and abundant micrites indicate that the Bahram Formation carbonates deposited on a ramp type carbonate platform, shallower southward. The most important diagenetic processes which affected the Bahram Formation carbonates are micritization, cementation, dolomitization, compaction, dissolution, fracturing, and calcitic veins formation. Cementation, dissolution, and dolomitization are the main diagenetic processes that affected the original texture. The abundant presence of bioclasts such as ecinoid, ostracod, and brachiopod together with geochemical analysis results such as low strontium content, low average of strontium/sodium ratio, high average of strontium/manganese ratio and low sodium content suggest that the primary mineralogy of carbonates were mainly calcitic. Paleoclimate conditions at the time of deposition seem to have been similar to climate of recent temperate regions. Investigation of the Middle-Late Devonian geographic maps reveals that the studied region which is located 30°S had been a part of Gondwana land so that geochemical results confirm this fact (Scotese 2014). In addition, the diagenetic and geochemical changes are indicators of long term effect of meteoric diagenetic fluids on the Bahram carbonates. So, it seems that the effect of meteoric diagenesis in north of the basin is greater than the south of it.

Keywords Bahram formation · Middle-Late Devonian · Eastern Iran · Carbonates · Microfacies · Diagenetic processes · Geochemistry

✉ Mahdi Hoseinabadi
mh_sedi_1355@yahoo.com

1 Department of Geology, Science and Research Branch, Islamic Azad University, Tehran, Iran

2 Department of Geology, Faculty of Science, Ferdowsi University of Mashhad, Mashhad, Iran

3 Department of Geology, Faculty of Science, University of Birjand, Birjand, Iran

4 Department of Hydrography, Faculty of Marine Science & Technology, Islamic Azad University-Tehran North Branch, Tehran, Iran

Introduction

The Bahram Formation was recorded for the first time by Ruttner et al. (1968) in Sartakht Bahram area (South of Ozbak Kuh). It consists of Middle-Upper Devonian blue-gray and black limestones with 300 m in thickness. Besides, the reference section of this formation was recorded from Shotori Mountains (southeast of Tabas) and includes hundreds of well-bedded gray limestones together with intercalations of shales, sandstones, and dolomites. Its upper and lower boundaries are continuously (conformable) in contact with the Shishtu and Sibzar Formations, respectively (Alavi-Naini 2009).

Eftekharnezhad et al. (1972) attributed the Kashmar Paleozoic rocks to Padeha, Sibzar, and Bahram Formations in the Kashmar quadrangle map (1:250,000 scale) which includes the study region. Bahari et al. 2006, studied the Upper Givetian-Frasnian corals of the Bahram Formation in south of Ozbak Kuh and concluded that these corals belong to reef settings and shallow open platform. Ahmadzadeh Heravi et al. 2007, studied the brachiopods of the Bahram Formation in Cheshmeh Shir section (Ozbak Kuh, northeast of Tabas).

In these previous works, little attention was paid to the sedimentology and geochemistry of the Bahram Formation. For this purpose, three stratigraphic sections from Bahram formation were studied, including: (1) Cheshmeh Shir (northeast of Tabas with 33° 34 10.8″ N, 57° 7 11.9″ E coordinates); (2) Kamar kuh (south of Kashmar with 35° 6 4.8″ N, 58° 26 44.4″ E coordinates); (3) Hozedorah (Southeast of Tabas with 33° 34 10.8″ N, 57° 7 11.9″ E coordinates) (Fig. 1).

This research attempts to: (1) reconstruct and discriminate depositional paleoenvironments of the Bahram carbonates in the three stratigraphic sections by means of microfacies recognition, (2) identify the diagenetic fabrics and processes that affected these carbonates and (3) analysis of major and minor elements in order to determine the geochemical properties of these carbonates with special attention to their primary mineralogy.

Methods

In this research, three sections of carbonate Bahram Formation rocks were studied in northeast of Cheshmeh Shir village (125 km from northeastern Tabas), Kamar Kuh section in 5 km from Eshaqabad village (south of Kashmar) and Hozedorah section, 65 km southeast of Tabas. The study includes field and laboratory investigations. So that, based on

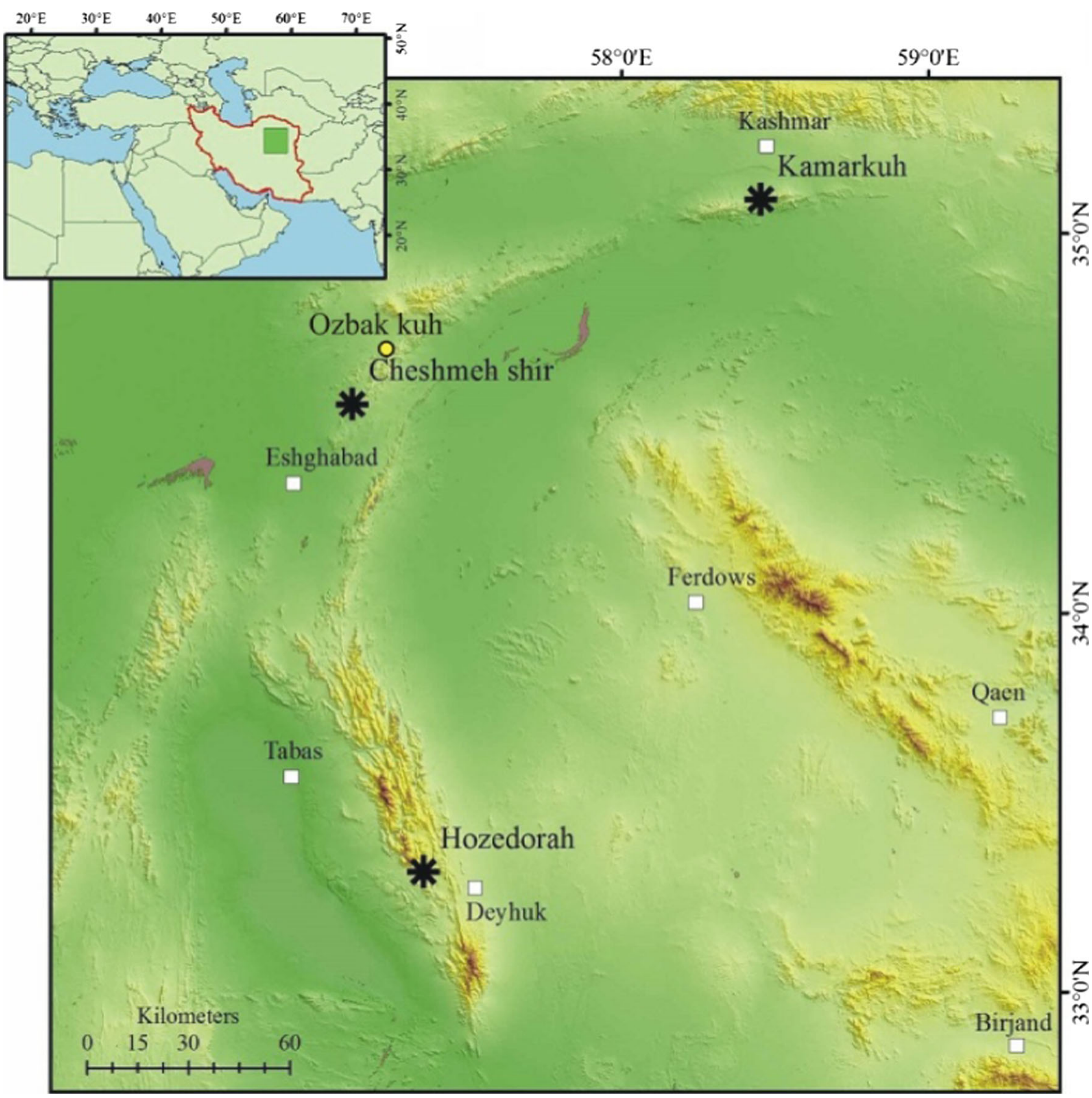

Fig. 1 A map showing location of the studied sections (*marked by star*). The location of type section at Ozbak Kuh village is shown as well

microfacies and textural changes that were observed in field investigations 97 samples from Cheshmeh Shir, 105 samples from Kashmar Kamar Kuh section and 92 samples from Hozedorah section were taken. In order to identify microfacies and interpret depositional environment, thin sections were prepared from all samples. The nomenclature of microscopic thin sections was done using Dunham (1962) and Embry and Klovan (1972) classifications.

In order to discriminate calcite and dolomite, all thin sections were colored by Red *Alizarin* and *Potassium Ferricyanide* following the scheme of Dickson (1965). Microfacies identification and depositional model interpretation were done based on Flügel (2010) and Wilson (1975) approaches.

After studying the thin sections, in order to identify major and minor elements and geochemical analysis, according to the El-Hefnawi et al. (2006) method, the values of insoluble materials in acid of the samples were measured. Those samples that the values of insoluble materials in their acids are less than 10 % were selected for geochemical analysis. A total of 52 samples with maximum micritic groundmass were selected for analysis.

Samples analysis was performed using Shimatzo-AA 670 atomic absorption spectrometer system in the chemical laboratory of Ferdowsi University of Mashhad. Major elements (calcium and magnesium) were measured by percentage and minor elements (iron, manganese, strontium and sodium) were measured by ppm. Also, cathodoluminescence photography was used in order to study diagenesis and history of cementation.

Stratigraphy

Kamar Kuh section

Kamar Kuh stratigraphic section with 188 m thickness is located in 5 km south of Eshaqabad village in Kamar Kuh (south of Kashmar). In this area, the Bahram Formation conformably covers the Sibzar Formation and is covered by Neogene deposits. This section is situated in the 1:100,000 geological map of Kashmar. This section mainly consists of gray to white limestones with intercalations of dolomite. The layers are mainly medium to thick bedded (0.1 to 0.3 m). Brachiopods and bivalves are the most abundant observed fossil of the section. Eight lithological units were recognized based on observed changes (lithology, color, lamination, etc.) (Fig. 2a).

Cheshmeh Shir section

Cheshmeh Shir stratigraphic section with 180 m thickness is located in northeast of Cheshmeh Shir village in 30 km northeast of Eshqabad (northeast of Tabas). Its lower boundary is conformable with the gray dolomite of the Sibzar Formation and its upper boundary is erosional. This section is situated in the 1:100,000 geological map of Ozbak Kuh. The study section commonly consists of dark gray limestones which are thin to thick bedded (0.05 to 0.8 m). Based on observed changes (lithology, color, lamination, etc.), ten lithologic units were identified (Fig. 2b).

Hozedorah section

Hozedorah stratigraphic section with 192 m thickness is located in 25 km of Deyhuk (southeast of Tabas). In this area, its lower boundary is conformable with Jamal Formation is continuous and is covered by Shishtu Formation. This section is situated in the 1:250,000 geological map of Boshruyeh. This section consists of gray to creamy limestones together with sandstone. The layers are mainly medium to thick bedded (0.2 to 0.8 m). Eleven lithological units were recognized based on observed changes (lithology, color, lamination, etc.) (Fig. 2c).

Microfacies (MF)

Bahram carbonates consist of variety of skeletal and non-skeletal grains, calcite cements, micrites, and early and late diagenetic dolomites. Skeletal grains are mostly crinoids/ecinoids, ostracods, brachiopods, and bryozoans. Non-skeletal grains consist mainly of peloids and intraclast.

Lithography analysis and investigations of 294 thin sections led to recognition of five facies.

Description of recognized microfacies from land to marine is as follows:

Shore face facies

Sub litharenite sandstone

Grains of this MF are moderate in sizes (300 to 500 μm), well sorted, and well and semi rounded. Abundance of quartz grains is up to 80 %. Color of this facies in the field samples is brown. Rock debris and feldspar content are very scarce. Intergranular calcitic and occasionally iron oxide cements are common (Fig. 3a).

Tidal flat facies

Mudstone MF with fenestral fabric

Fossil contents of this MF are scarce and include brachiopod debris; lime mud is the main framework of the rock. The main characteristics of this MF are the presence of sparry calcite, fenestral fabric or birdseyes (about 3 %), and fine rhombohedra of dolomite. Fenestral fabric or birdseyes are the small

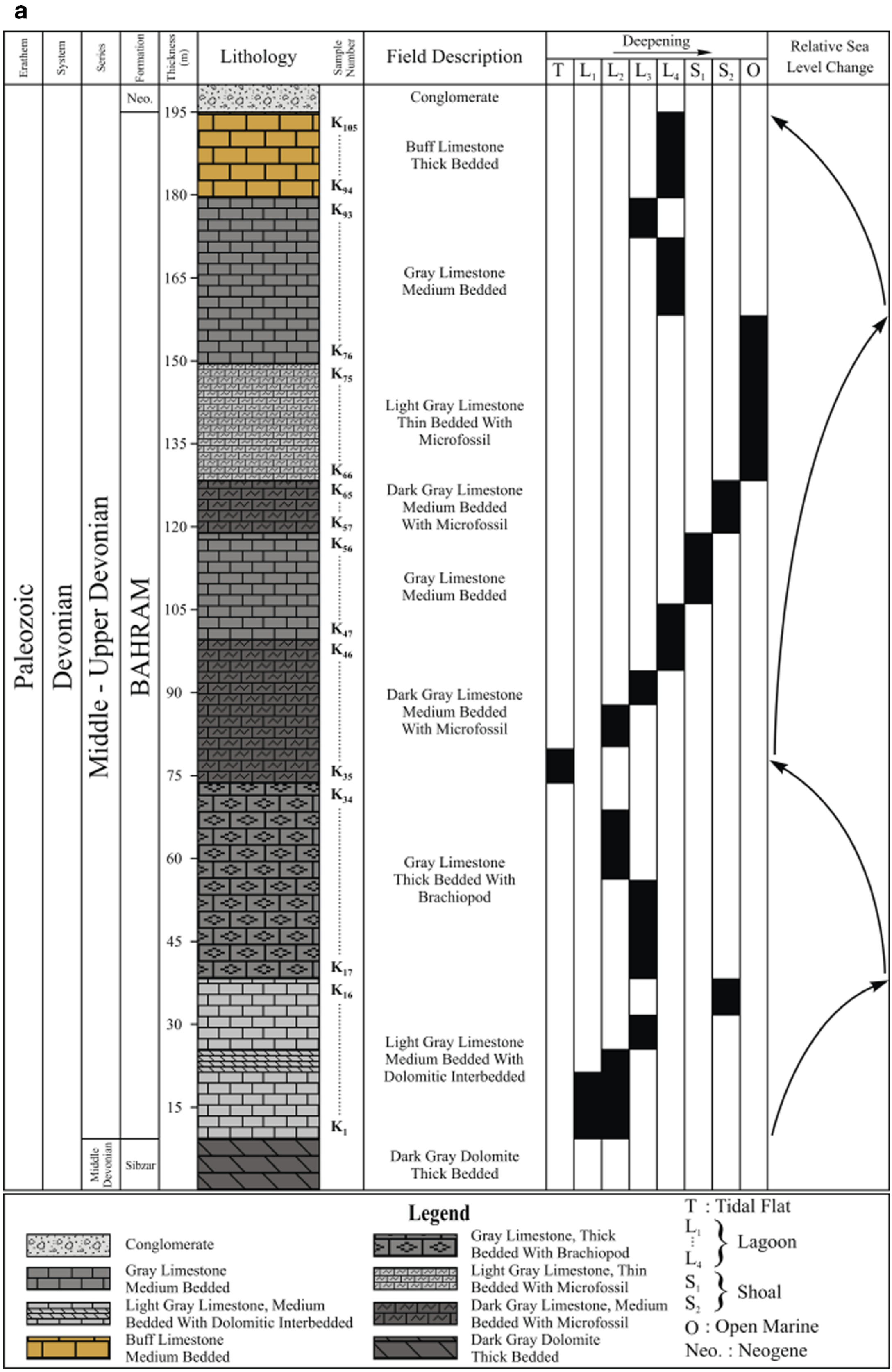

Fig. 2 **a** Stratigraphic sequence and vertical facies changes in Kamar kuh section. **b** Stratigraphic sequence and vertical facies changes in Kamar kuh section. **c** Stratigraphic sequence and vertical facies changes in Hozedorah section

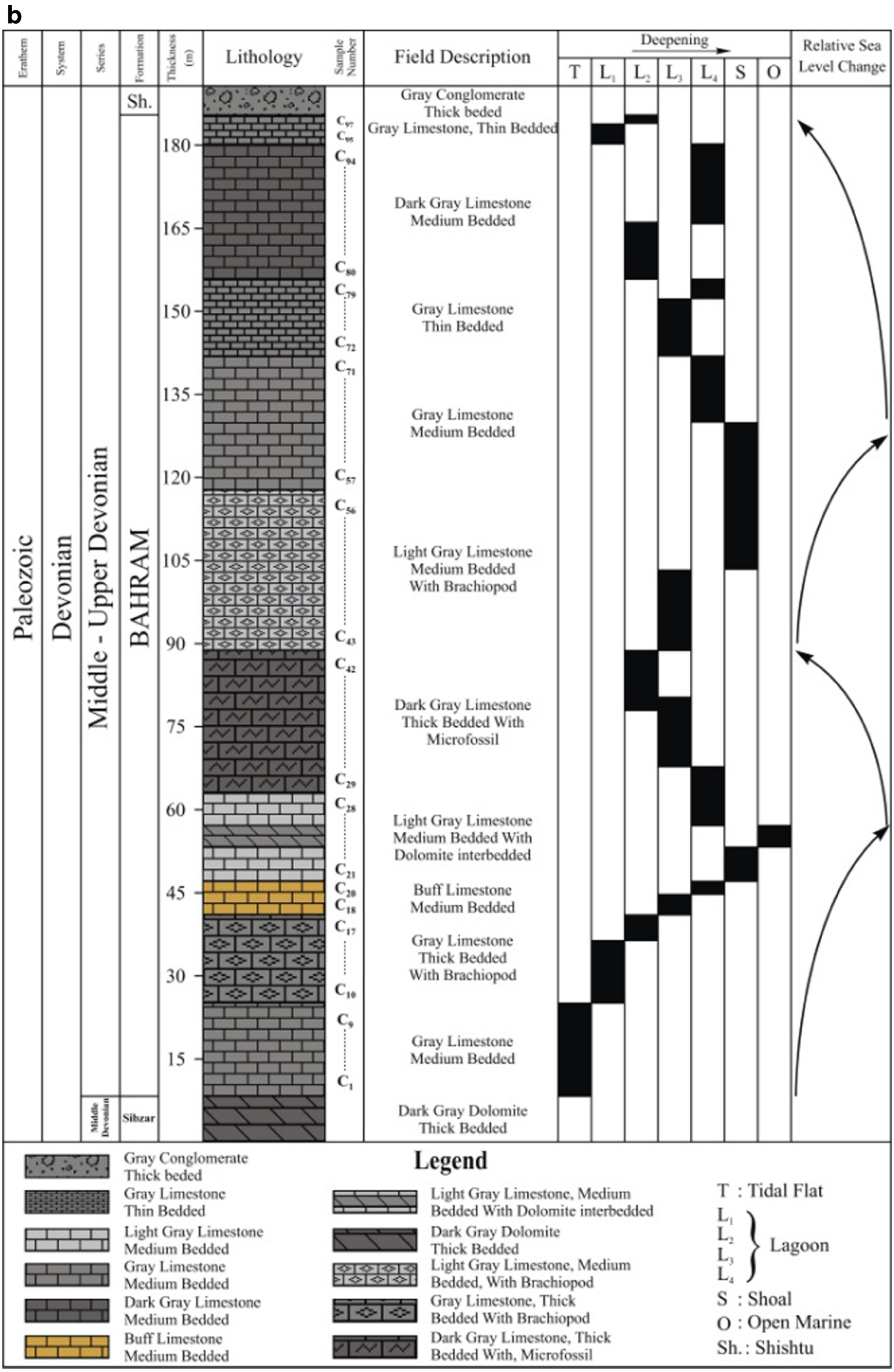

Fig. 2 (continued)

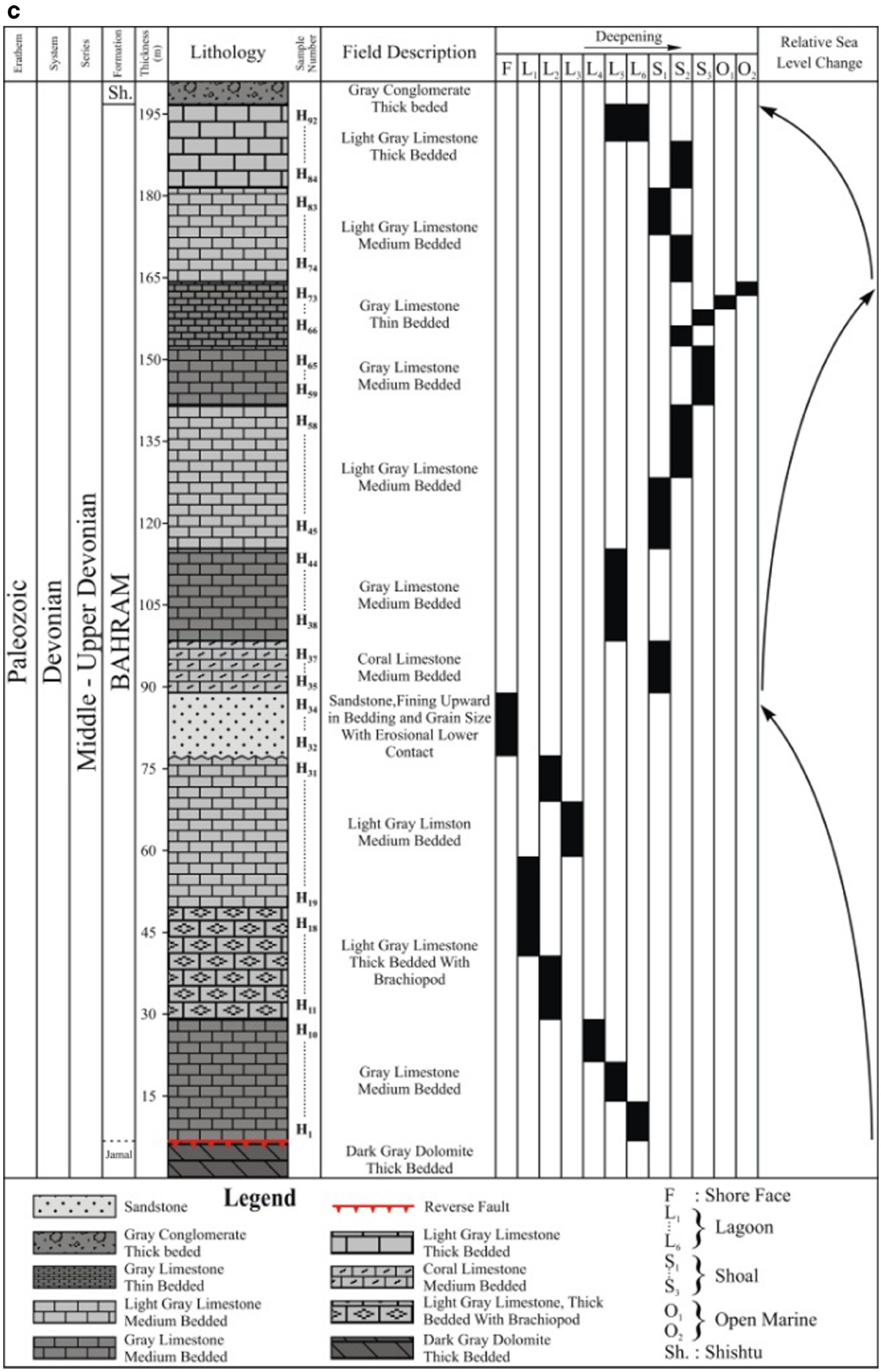

Fig. 2 (continued)

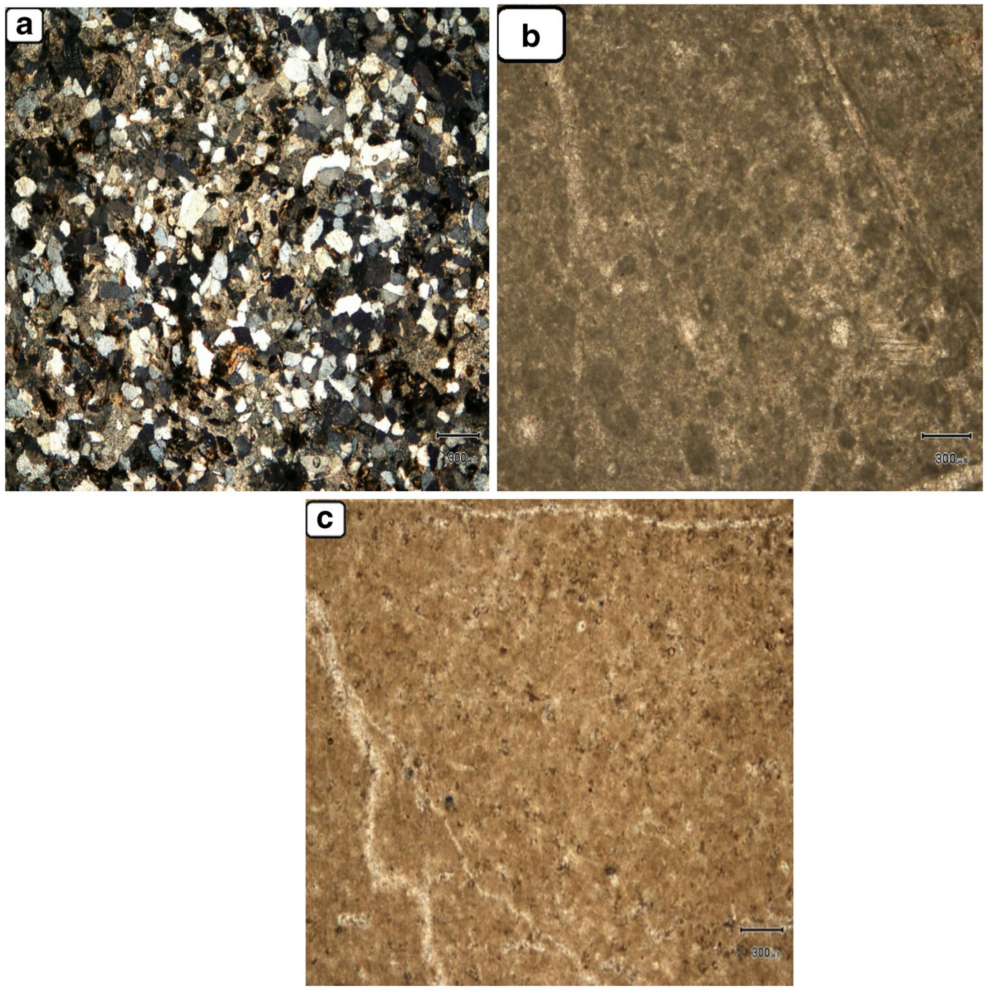

Fig. 3 Microfacies of shore face and tidal flat environments of the Bahram Formation in the study sections. **a** Sub Litharenite MF **b** Mudstone MF with Fenestral Fabric, **c** Dolomitic Mudstone MF

millimeter-sized voids which form in upper tidal deposits due to shrinkage and expansion, formation of gas bubble and captured air through shrinkage of the algae mass (Flügel 2010). Existence of Brachiopods debris with no observation of intact fossils in the region indicates tidal action for carrying them from ocean. The presence of fine to moderate dolomite crystals together with fenestral fabric suggest near surface formation of this dolomite during early diagenesis in upper tidal flat to tidal flat environments (Lasemi et al. 2012). The presences of quartz grains are indicative of the proximity of this MF to the land (Fig. 3b).

Dolomitic mudstone MF

Lack of skeletal components in this facies is an indicator of the absence of favorable conditions for existence of extant organisms (Flügel 2010; Brasier et al. 2011; Immenhauser et al. 2012). The presence of fine-grained dolomite suggests near surface formation of this dolomite which occupies more than 30 % of groundmass during primary stages of diagenesis in tidal flat. Also, the absence of noticeable skeletal and non-skeletal components and the presence of micritic groundmass are indicators of low energy in the deposition setting of this MF (Gregg and Shelton 1990; Adabi 1996) (Fig. 3c).

Lagoonal facies

Mudstone MF

Skeletal and non-skeletal allochems in this MF are very scarce (1–2 %) and micrite is the main component. The absence of fossil is an indicator of limited water circulation and absence of favorable conditions for existence of organisms (Bosence and Wilson 2003; Sandullia and Raspinib 2004; Palma et al. 2007).

Because of high amount of lime mud, lack of subaerial exposure evidence, and the absence of skeletal and non-skeletal components, deposition of this MF likely occurred in shoreward parts of the lagoon (Fig. 4a).

Bioclastic wackestone MF

Ostracod debris form 30–35 % of the MF and are the main components. Other skeletal components are brachiopod,

Fig. 4 Microfacies of lagoonal environment in the study sections. **a** Carbonate mudstone MF **b** Bioclastic wackestone MF **c** Peloidal wackestone MF **d** Peloidal packstone/grainstone MF

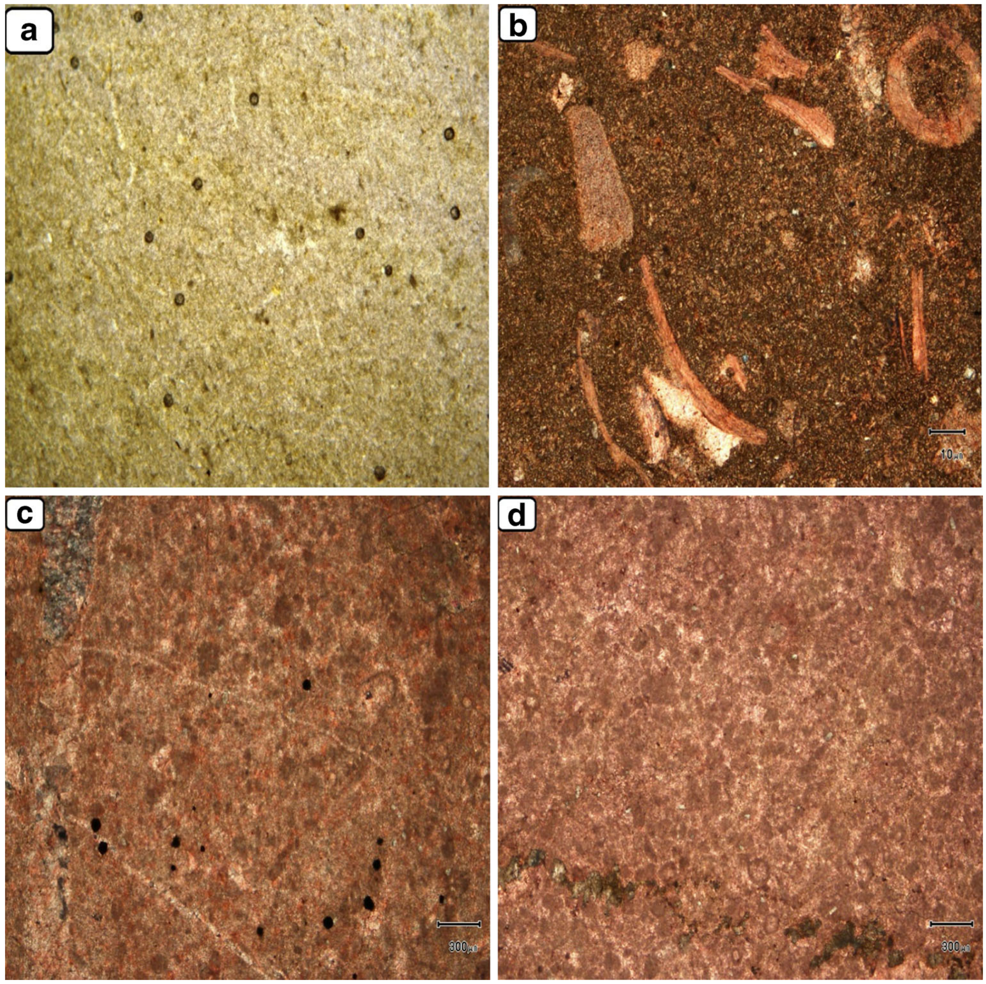

miliolid, bivalve and gastropod in minor amounts. Non-skeletal peloid debris (3–4 %) are present in micritic groundmass. Bioturbation phenomenon, geopetal, micritization, as well as stylolites are observed (Fig. 4b).

Peloidal wackestone MF

Peloids with up to 40 % abundance are the main components of this MF. These allochems are well sorted and well rounded. Skeletal debris such as ostracod, brachiopod, bivalve, and echinoid occurred in the micritic groundmass with less than 5 % abundance. Because of the low amount of bioclast and presence of peloids, depositional environment of this MF can be attributed to a low-energy lagoon with limited connection to open marine (Tamasovych 2004) (Fig. 4c).

Peloidal packstone/grainstone MF

Peloids with 60 % abundance and moderately sorted grains are the main components of this MF. Intraclasts with about 4 % abundance and brachiopod and ostracod debris with 2 % abundance are other components. The spaces between allochems are filled with sparry calcite. Hematitization and stylolitization are the observed diagenesis phenomena in this MF (Fig. 4d).

Shoal facies

Bioclastic grainstone MF

This MF shows the most energetic deposit in the study succession. The absence of muddy matrix is indicative of high energy of the environment. Shoals with lateral extension were not observed, so they have probably existed in the form of patches (Flügel 2010).

The abundant occurrence of skeletal components such as echinoderm and crinoids (50–70 %) and appearance of bryozoan (15 % and in large size) show that this MF deposited in proximity of open marine (Wilson 1975; Geel 2000). The space between allochems is filled mainly by Equant mosaic cement.

Concentration of echinoderms in the middle ramp environments is common (Flügel 2010) (Fig. 5a).

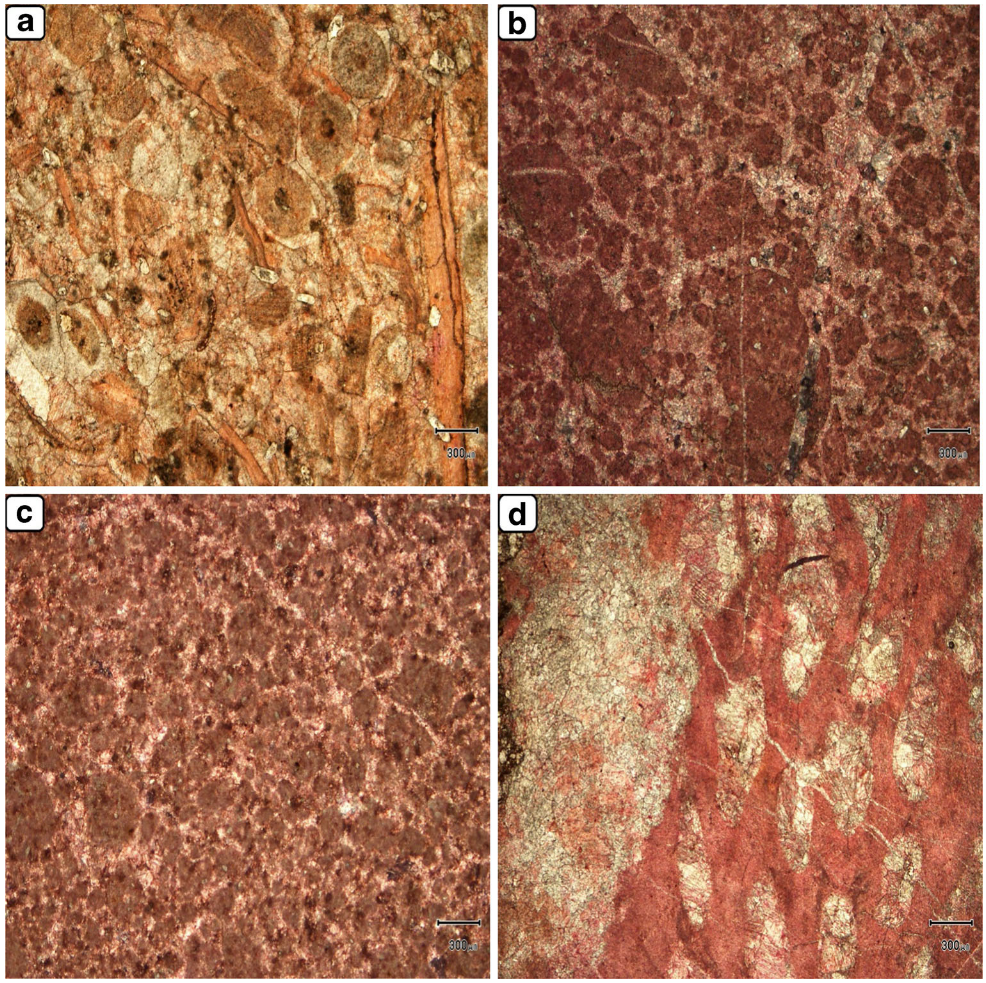

Fig. 5 Microfacies of shoal environment in the study sections. **a** Bioclastic grainstone MF **b** Intraclastic grainstone MF **c** Peloidal grainstone MF **d** Coral boundstone MF

Intraclastic grainstone MF

The most typical allochems of this MF are intraclasts with 10 to 40 % abundance, and 0.5 to 1 mm in diameter. These intraclasts are moderately sorted and mainly micritized. Other constituents are non-skeletal components such as peloid with 8–10 % abundance, skeletal fragments such as brachiopod with 4 % abundance and terrigenous quartz grains with about 1 %. Mostly all of the groundmass is composed of isometric mosaic cement. On the basis of the presence of sparry cement groundmass, absence of micrite, moderately large intraclasts, and open-marine skeletal particles, the sharp increase of the environment energy, this MF likely deposited in tidal channels (Flügel 2010) (Fig. 5b).

Peloidal grainstone MF

Well-rounded peloids with about 50–60 % abundance and 0.2–0.4 mm in size are the main components of this MF. Other components are intraclasts with 5–7 % abundance and skeletal fragments such as brachiopod with 3 % abundance. Since grain supported peloids are deposited in low-energy environment, the presence of this MF *in shoal* (field observations have shown that these facies does not have enough lateral extension, so they are considered as shoal) is attributed to reworking from low-energy environment through tidal channels crossing the middle ramp and then the micrite is removed and the cement is precipitated (Tucker and Wright 1990; Carozzi 1989) (Fig. 5c).

Coral boundstone MF

This MF is composed of Stromatoporoids, the chambers of which are filled by Fe-calcite cement and Fe-free calcite cement. Boundstones are formed in high-energy environments (shoal) above wave base (Fig. 5d).

Open-marine facies

Bioclastic rudstone/floatstone MF

Brachiopod with 20 % abundance and up to 5 mm in size, bryozoan with 15 % abundance and average size of 4–5 mm, echinoderm with 60–70 % abundance and average size of 2–

3 mm are the main allochems of this MF. The spaces between bryozoans are filled with Fe-calcite cement and dolomite. Skeletal components are mostly well preserved, and sometime broken. Echinoderms commonly live in open-marine environments, in sand shelf or through shore line, and in abyssal deeper waters (Tucker 2001). On the basis of the above-mentioned reasons, the presence of brachiopods, abundance of mud, and absence of green algae (Badenas and Aurell 2009). depositional setting of this MF is attributed to low-energy open marine below the wave base (Fig. 6a).

Bioclastic echinoid packstone MF

The main components of this MF are echinoderm fragments with 50–60 % abundance and 1–2 mm size, which mainly encompassed by syntaxial overgrowth cement. Subordinate allochems are brachiopod and bryozoans with 7 % abundance and 1 mm size, about 2 % terrigenous quartz grains, about 1 % opaque minerals. Also, dolomitization and hematitization are observed in this MF (Fig. 6b).

Existence of skeletal debris of stenohaline skeletons like echinoderm and bryozoan which is mainly dependent of salinity and textural characteristics is a good indication that these two microfacies were formed on open-marine region (Holcova and Zagorsek 2008; Saber 2012).

Depositional model of the Bahram formation in the study successions

Determination of the sedimentary facies assemblage is the most important factor for paleoenvironment reconstruction, which is usable for recognition of climatic changes and sedimentary basins history. Based on the presented evidences, depositional conditions of each facies assemblage, and their vertical relationship (Fig. 2a, b, c), Walther Law (Middleton 1973). absence of reefal facies, slumping and sliding facies, gradual deepening trend from the shallow platform to the basin, absence of the special grains of carbonate shelf such as cortoid, oncoid, pisoid, and aggregate which are rare in the carbonate ramps (Einsele 2000; Flügel 2010). the depositional settings of the successions could be attributed to a carbonate platform (homoclinal ramp type). Carbonate ramps were common through all of the geological records, but they are developed whenever reef-forming organisms are absent or unable to grow. Limited expansion of reefs in carbonate ramps in proportion to rimmed carbonate platforms is the characteristics of the ramp (Einsele 2000).

Inner ramp and the mid ramp are two main depositional environments of the Bahram Formation in the study sections (Fig. 7).

Based on recognized facies and their distribution patterns in the study sections, the depth of the ramp reduced from north (Kamar Kuh section) toward south (Hozedorah). Besides, barrier facies belt is more developed in Hozedorah section because of the presence of coral Boundstone.

Diagenesis

Diagenesis includes all of the physical, chemical and biogenic processes which affect the sediments that occur after the sedimentation to the beginning of metamorphism in marine, meteoric and burial environments (Tucker and Wright 1990). Commonly diagenesis processes affect the sediments physically and chemically and are controlled by different processes including: biogenic activities and bioturbation by extant organisms (Kasih et al. 2008). effect of organic acids (Heydari and Wade 2003). purity of sediments, mineralogy of sediments, chemical properties of intraporous fluids, geomorphologic position, geographical factors, rate of deposition, and tectonics (Tucker and Wright 1990). On the basis of the

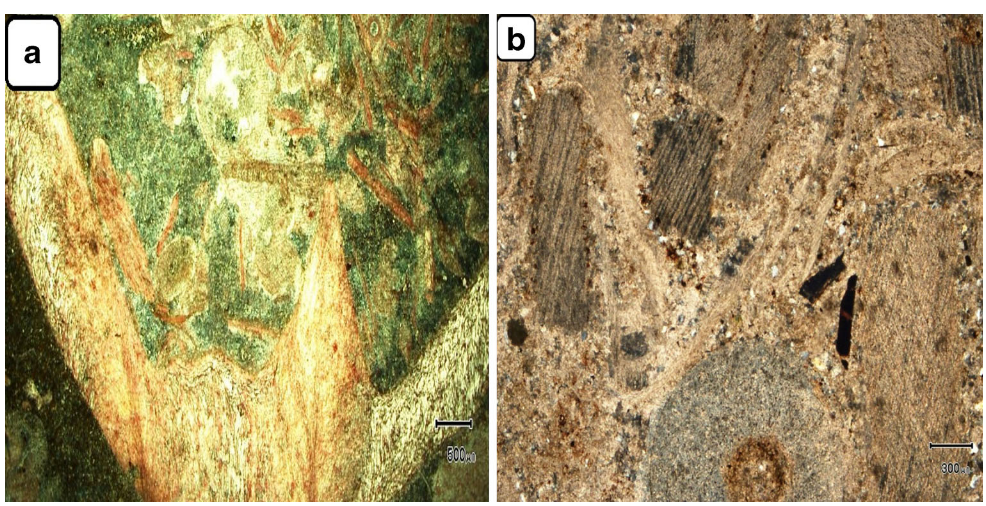

Fig. 6 Microfacies of open-marine environment in the study sections. **a** Bioclastic rudstone/floatstone MF **b** Bioclastic echinoid packstone MF

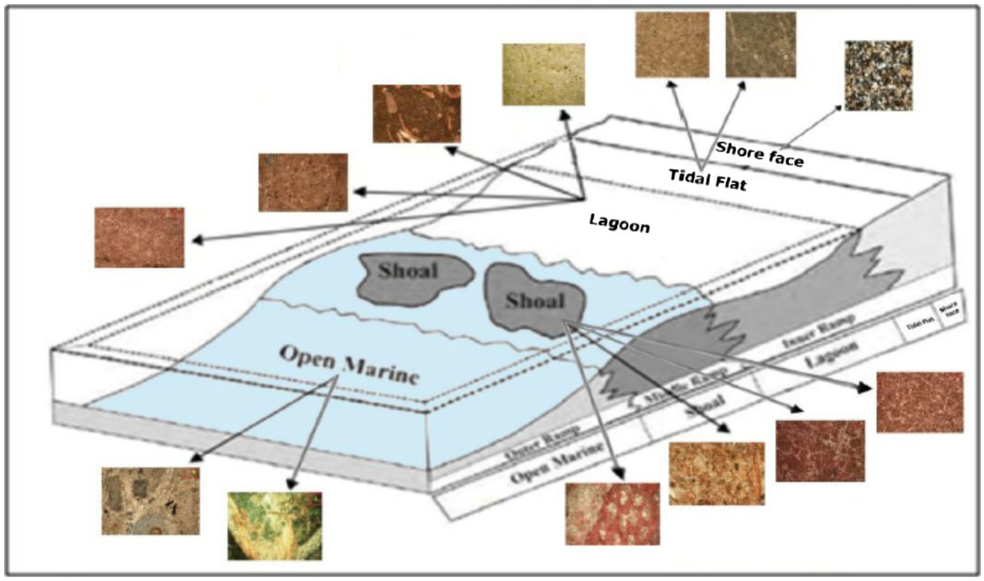

Fig. 7 Depositional model of the Bahram Formation in the study regions

microscopic analysis on thin sections of the Bahran Formation carbonates, types of diagenetic fabrics and processes, type of diagenetic environments and paragenetic successions were presented. These processes include micritization, bioturbation, geopetal fabric, cementation, dissolution, dolomitization, compaction, fracturing and filling by sparry calcite, silicification and hematitization. Distribution of diagenetic phenomena in different sections is almost similar and no clear difference is observed.

Micritization

Micritization is a process which occurs at the first stages of marine diagenesis and in the boundary of water and sediment (Samankassou et al. 2005). This process occurs due to frequent activities of micro-organisms such as cyanobacteria, algae, and fungus on the surface of allochems (Garcia-Pichel 2006; Carols 2002; Vincent et al. 2007). Then, due to filling of these cavities (holes) by micrite, a micritic cover forms around the particle (Khalifa 2005) and is indicative of low deposition rate. This process is observed in the Bahram Formation on the allochems such as brachiopods, bivalves, and crinoids and especially in the bioclastic wackestone microfacies in lagoon environment (Fig. 8a).

Diagenetic fabrics

Bioturbation

Bioturbation fabric is indicative of spatial arrangement and geometry, abundance, texture, and filling of the holes due to activities of mud-feeder organisms. Such holes are formed by boring in the moderately hard sediments. Boring is a typical process in recent subtidal environments, which mostly cause the absence of internal layering (Flügel 2010). Bioturbation is controlled by some factors such as sea level changes, carbonate production rate, status of the substrate surface, rate of colonization in substrate surface. The identification criteria of bioturbation in the study samples are the mottled appearance and their texture and color are different with groundmass. This fabric is recognizable in lagoonal wackestone facies (Fig. 8b).

Geopetal fabric

Geopetal fabrics indicate the relationship between top and bottom of the layer at the time the rock was formed. Recognizing geopetal fabrics in limestones is crucial for understanding the depositional and post-depositional history of carbonate rocks, particularly changes in original sedimentary dips of beds by compaction and tectonic tilting of beds. (Flügel 2010). In the study samples, this fabric is observed in the skeletal grains and also in some holes. This fabric is recognizable in lagoonal bioclastic wackestone facies (Fig. 8c).

Cementation

Cementation is one of the most important diagenetic processes, which besides the physical and mechanical effects on the rock, present well indicatives concerning trend of the diagenesis and diagenesis environments. Calcite cements and sometime dolomite cements are observed in the study thin sections. The most important fabrics in these samples are shown in the following sections.

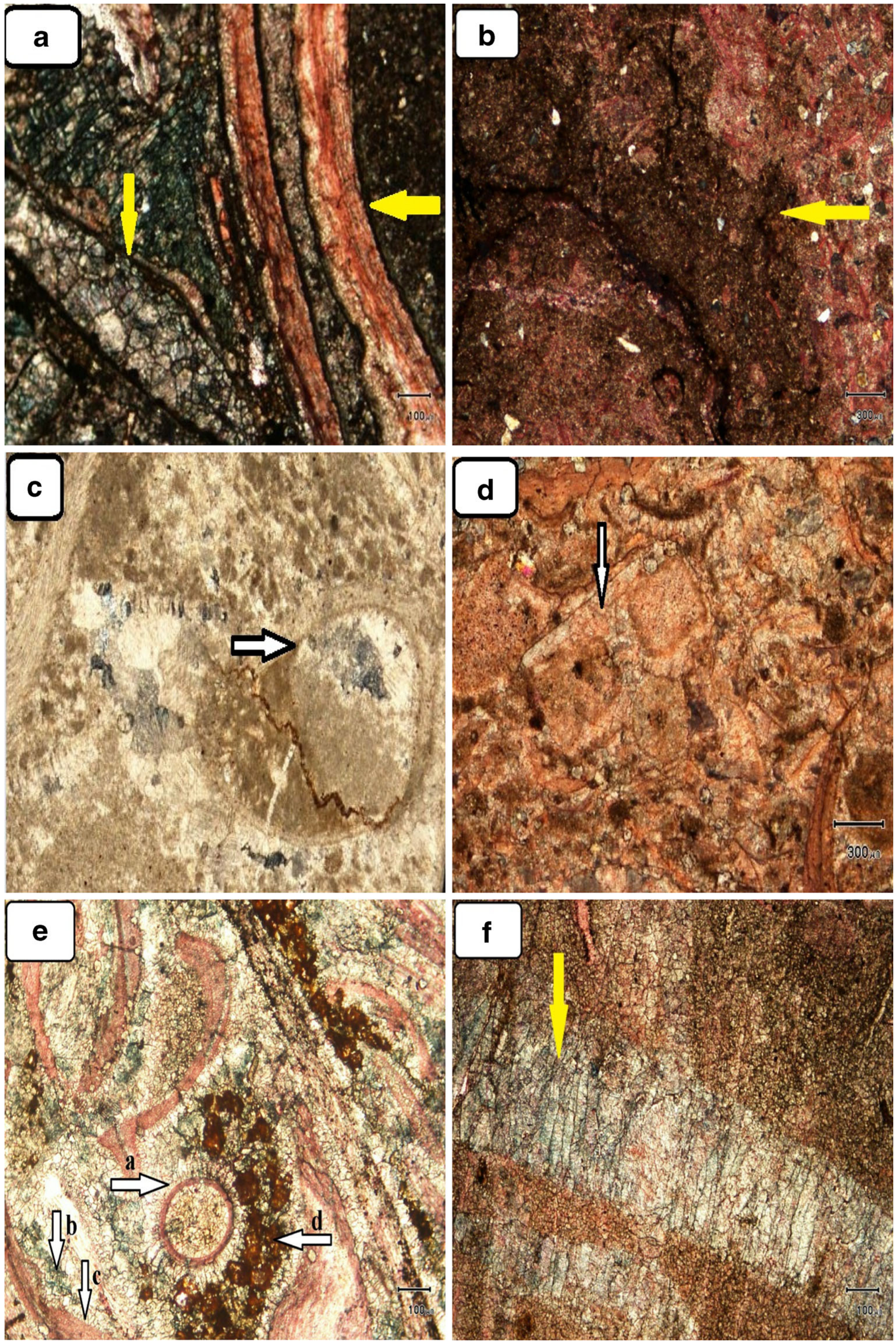

Fig. 8 Diagenesis fabrics and processes of the Bahram Formation carbonates **a** Micritization which affected brachiopod as a dark micritic envelope (*yellow arrow*). **b** Bioturbation which caused to turbation of the sediment (*yellow arrow*). **c** Geopetal fabric. **d** Syntaxial overgrowth cement which grew around echinoderm and show light continuity (arrow). **e** (*a*) Isopachous rim (blade) cement around brachiopod spine; (*b*, *c*): Fe-calcite cement (blue) and Fe-free calcite cement respectively, this change is indicative of deep burial (thin section colored) and d: dolomite large crystals **f** Dog tooth pore fillings composed of Fe-calcite cement (yellow arrow). **g** a: Equant mosaic cement and b:hematitization (*green arrow*). **h** Drusy calcite cement. **i** Blocky cement **j** (*a*) Pore filled by calcite mosaic cement and (*b*) fracture originated porosity which filled by calcite cement. **k** (*a*) Stylolitization originated porosity which is preserved (*yellow arrow*). **l** Intra-particle porosity which is filled by calcite mosaic cement. **o** Hematitization in the bryozoans chambers (*yellow arrow*) **p** Neomorphism

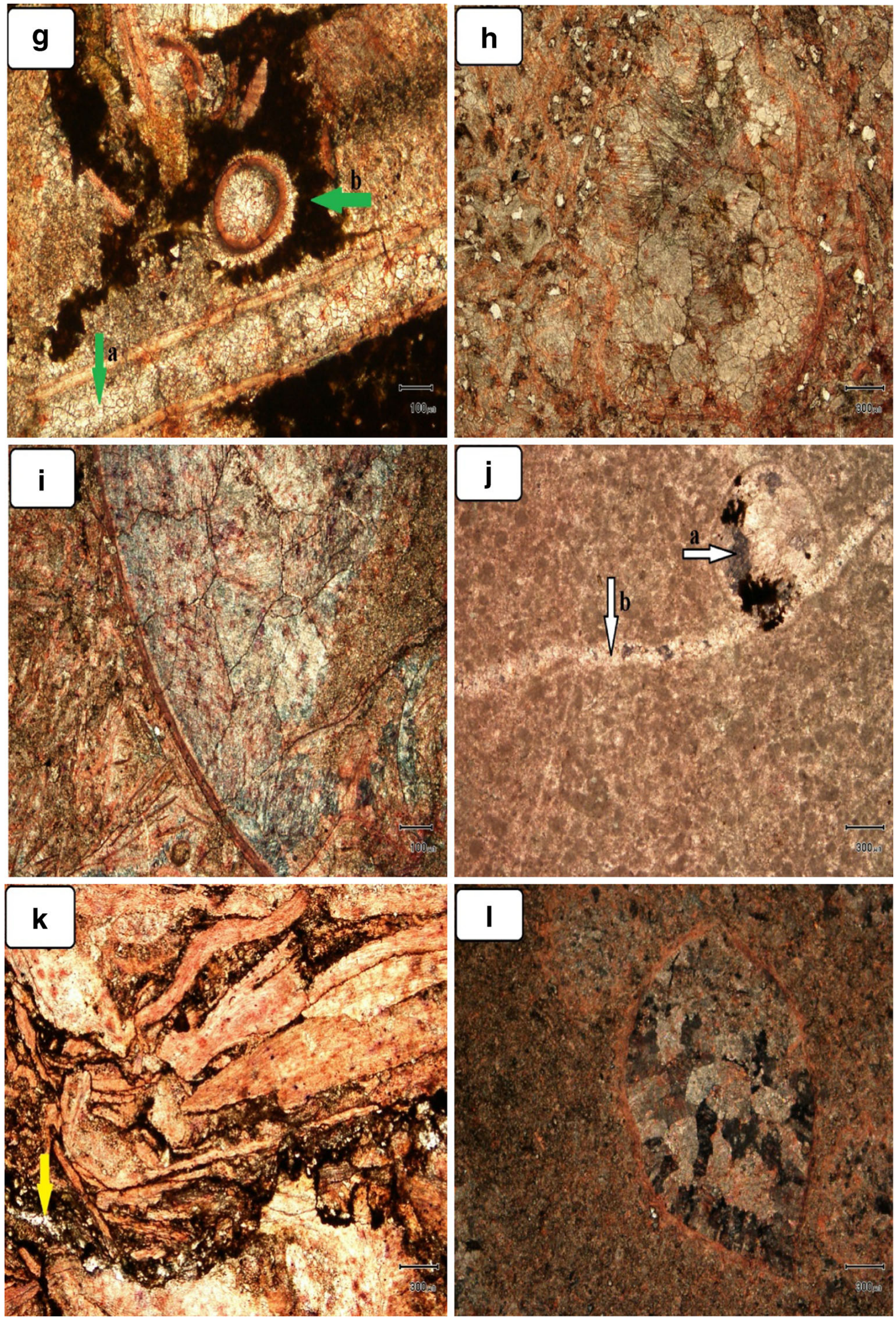

Fig. 8 (continued)

Syntaxial overgrowth cement

This cement is very developed in the study samples because of abundant unbroken and fragmented echinoderm. This cement is transparent and occasionally dusty in the barrier and open-marine subenvironments facies, particularly in bioclastic grainstones and bioclastic echinoid packstones. The size of this crystal sometimes reaches to about 200 µm and is dominantly present in packstones and grainstones microfacies.

Cathodoluminescence microscopic studies on these cements are indicative Syntaxial cement with light luminescence is observable around echinoderm indicating meteoric conditions (Figs. 8d and 10a).

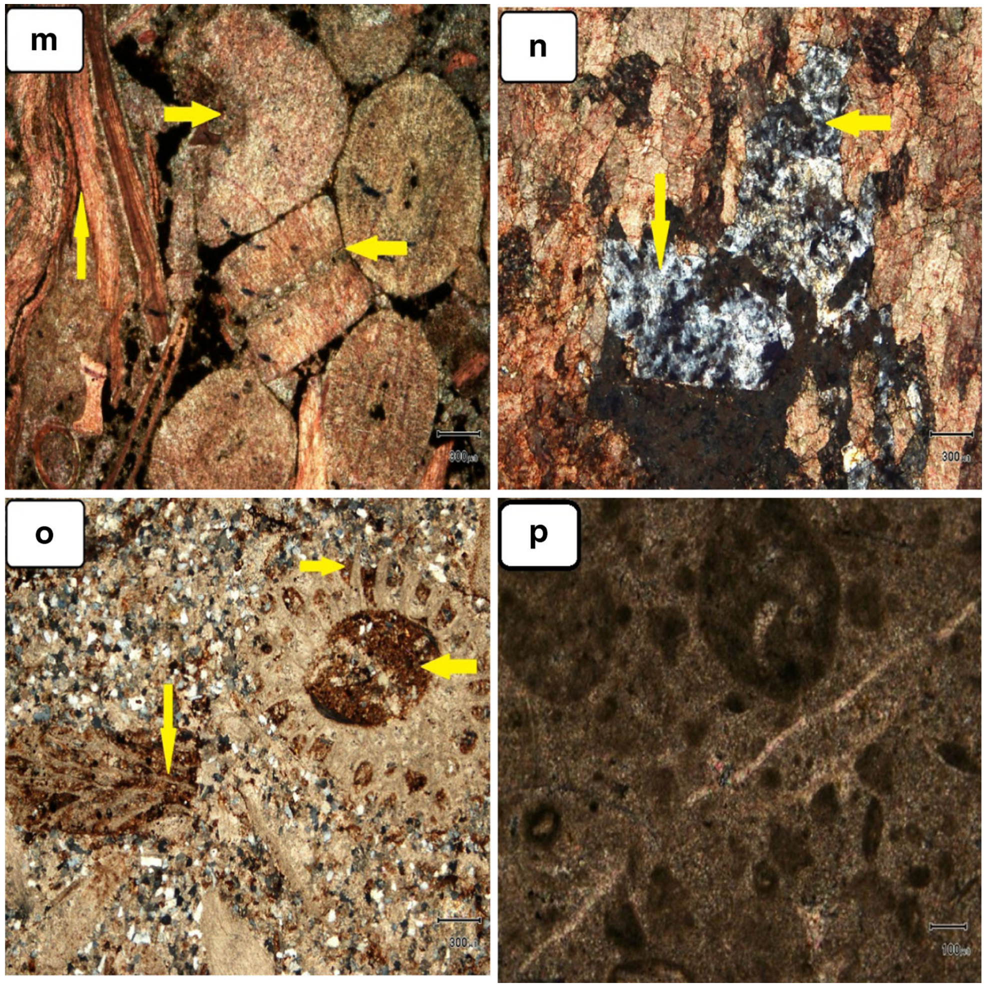

Fig. 8 (continued)

Isopachous rim cement

Isopachous rim cement commonly is formed in needle shapes and around grains and pores (Haijun et al. 2006). This type of cement might have been formed during low rate of sedimentation in the marine environment and was probably formed after micritization before high compaction (Sanders 2001).

Saturation of sea water from calcium carbonate in a quiet setting is essential to form this type of cement. It is formed isopachously around the grains (Longman 1980; Ehrenberg et al. 2002). This type of cement is observed in study samples especially around the brachiopod spines (Figs. 8e and 10a).

Dog tooth cement

They are triangle or rhombus ferroan calcite minerals, which grows in grain walls or on primary cement commonly or semi-commonly. This type of cement grew on surface of the allochems in the study samples, and it is formed likely during the rising stage (Fig. 8f).

Equant mosaic cement

This type of cement consist of subhedral calcite crystals with various sizes ranging from 50 to 60 μm. This type of cement commonly is formed after the lithification and bearing compaction in burial settings after the deposition of the primary cement, it is considered as secondary cement (Flügel 2010). This cement filled the moldic and intra-particle porosities in the study samples (Fig. 8g).

Drusy calcite spar cement

Drusy calcite spar cement is characterized by increasing in size of crystals toward the center of pores or voids (Flügel 2010). This cement is observed in the study samples as a filling in veins and solved porosities. Meteoric origin is likely for this cement (Figs. 8h and 10g).

Blocky cement

Blocky cement is calcite cement consisting of medium to coarse-grained crystals without a preferred orientation and often shows distinct crystal boundaries. This cement is mostly considered as a secondary- or third-generation cement and causes filling of the pores. Blocky crystals have various sizes (300–500 μm).

This cement is formed in burial environments besides meteoric environments (Tucker 2001; Flügel 2010) (Fig. 8i).

Neomorphism

This process usually takes place in the presence of water and hence is a wet process (Tucker and Wright 1990). The neomorphism may change the micrite partially or totally to sparite or pseudosparite. It could be a useful process that preserves the original shape of the fossil shells through changing the aragonite of their original shells into calcite during this process that is called calcitization (Tucker 2001). (Fig. 8p).

Dissolution

The dissolution patterns can be traced on both macroscopic and microscopic scale. Dissolution process occurs under condition that pore fluids, which are in contact with sediments, are under saturation in relation to calcium carbonate. This process occurs mainly near surface diagenetic environments. However, it may also occur during deep burial (Tucker 2001) in relation to mineral dissolution capability, so that low Mg-calcite has a low dissolution capability in proportion to high Mg-calcite and aragonite. Also, calcite is more unstable than dolomite. In the study samples, dissolution process had a basic effect in porosity formation and it is the main factor to form moldic, intragranular, intergranular pore, fracture, and channel porosities, which are filled by cement in the later stages of diagenesis. The observed porosities mainly include fracture and channel porosities, so that dissolution through some fracture and stylolites expanded channel porosity. It is worth mentioning that channel porosity raised from stylolites is the only preserved porosity in the study section (Fig. 8l, k, j).

Dolomitization

Dolomites in the carbonates have different origins.

Based on size, recognized dolomite from the study samples are of four types (D1 to D4).

- Very fine to fine dolomite crystals:
  The D1 dolomites are non-luminescence crystals with no allochem in between (15–50 μm) which are formed in tidal flat and near-surface environments. It is known as early diagenesis dolomite (Gregg and Shelton 1990; Adabi 1996).
- Fine to medium dolomite crystals:
  The D2 dolomites are pervasive in mudstone, wackestone and packstone with crystal size ranging from 40 to 200 μm. They are subhedral to euhedral dolomites with planar boundaries, dolomites which filled the space between allochem as cement.
- Medium to coarse dolomite crystals:
  The D3 dolomites are euhedral with planar boundaries and zoning which is observed as single, sporadic, and dense crystals through stylolites and surfaces of some allochems (100 to 250 μm).
- Adjacent dolomites (crystal size more than 300 μm) of stylolites are formed during the late diagenesis (Figs. 8e and 10a, c).

Dolomites in the carbonates have different origins. D1 based on absence of carbonate grains, non-luminescence and fine crystal has been formed in intertidal to supratidal environments. Other dolomites (D2, D3, and D4) based on petrographic evidences such as zoning; planar boundaries and increase in crystal size are replacement types (Reinhold 1998). Zoning in these crystals can be related to changes in the composition of dolomitizing solution (Johnson et al. 2009). Dull and bright zonation in our samples (D3 and D4 especially) are also related to the presence of the main activator Mn^{2+} and quenchers Fe^{2+} or lattice defects (Teedumae et al. 2006; Touir et al. 2009).

Compaction

Compaction includes all processes that reduce the volume of the rock masses (Flügel 2010). This process causes closer arrangements of grains, their fractures, and their possible pressure solution where the grains are in contact with each other. This is related to deposition rate, burial depth and volume of sediments (Einsele 2000). There are some evidences from mechanical and chemical compaction in the study samples.

- Mechanical compaction
  This type of compaction commonly begins immediately after sedimentation and causes to sediment compaction, closer arrangement of grains, omitting intergranular water and porosity reduction. This process is observed in the study samples as fractures, fragmentation, point and tangential contact of skeletal grains, peloids as well as sliding of grains.
- Chemical compaction
  This type of compaction occurs in deeper condition and higher temperature in relation to mechanical compaction. Concave-convex intergranular contact and stylolites

are the main evidences of this type of compaction in the study samples. Stylolites occur in deeper conditions in proportion to concave-convex intergranular contact, and it is one of the especial evidence of the burial diagenesis environments. During this process, essential material for burial cement formation is provided (Tucker and Wright 1990; Lambert et al. 2006). In some of the samples, stylolites acted as a channel for the motion of dolomite forming fluids and caused to form dolomite through stylolites (Fig. 8m).

Although physical compaction may take place during the early stage of diagenesis (Jadoul and Galli 2008; Ronchi et al. 2011). but the chemical compaction occurs during mesogenesis stage. This is indicated by the presence of diverse forms of stylolites in samples.

Silicification

Silicification can occur during the early or late diagenesis. The presence of terrigenous quartz grains after dissolution may be indicative of silica source for silicification process. Saturation of the inter-porous fluids with silica and domination of acidic conditions is essential for replacement and deposition of silica in carbonate (Maliva and Siever 1988) (Fig. 8n). Silicification process is observed commonly in fossils and brachiopod fragments.

Hematitization

This process is observed in the study samples through stylolites, as filling in the bryozoan chambers, replacement in brachiopod, and carbonate mud smearing. More likely during the sediments uplift, Fe ions penetrated into sediments via meteoric waters and fractures, and they converted to hematite under oxidizing conditions through time. This process rather occurred during the late diagenesis (telogenesis) (Fig. 8o).

Fracturing and filling by sparry calcite

Fracturing is controlled by some factors such as lithological properties, grain sizes, layer thickness, and stratigraphic characteristics including facies, depositional cycles and diagenesis (Cook et al. 2006). Tectonic processes are able to increase the

Fig. 9 Paragenesis succession of the Bahram Formation carbonates in the study sections

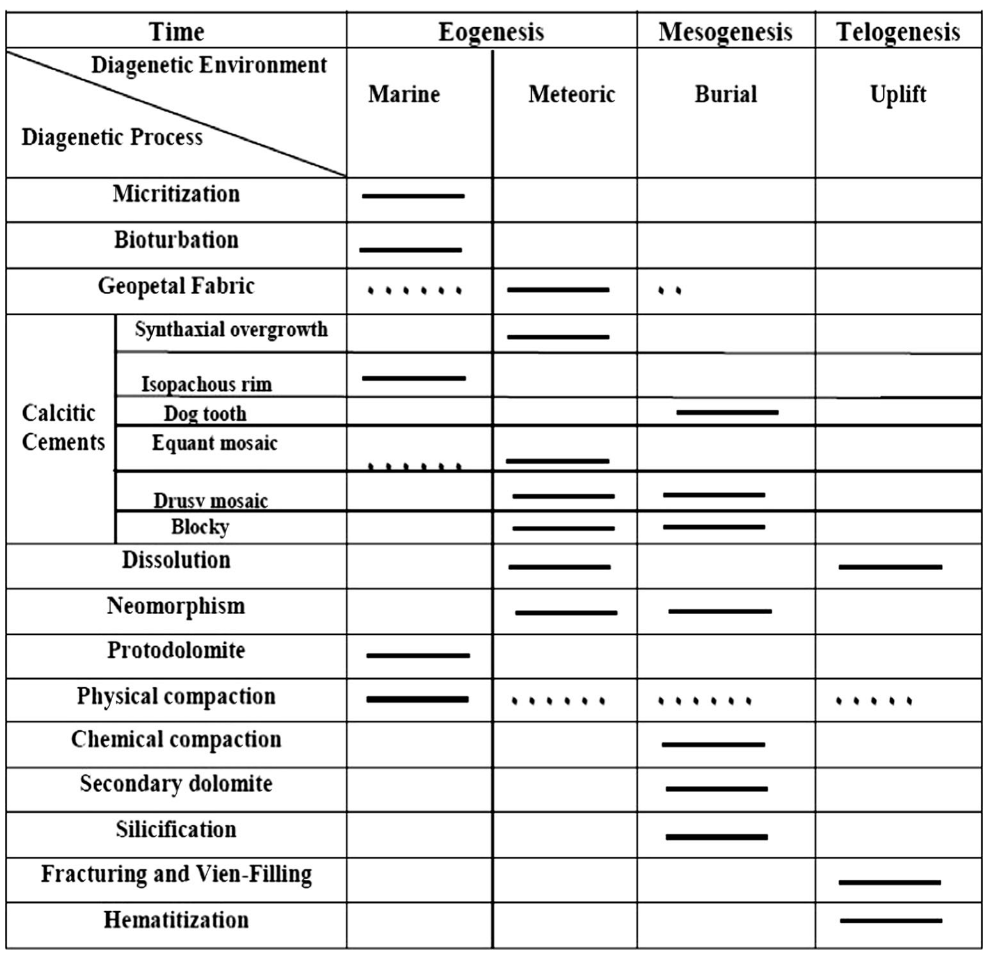

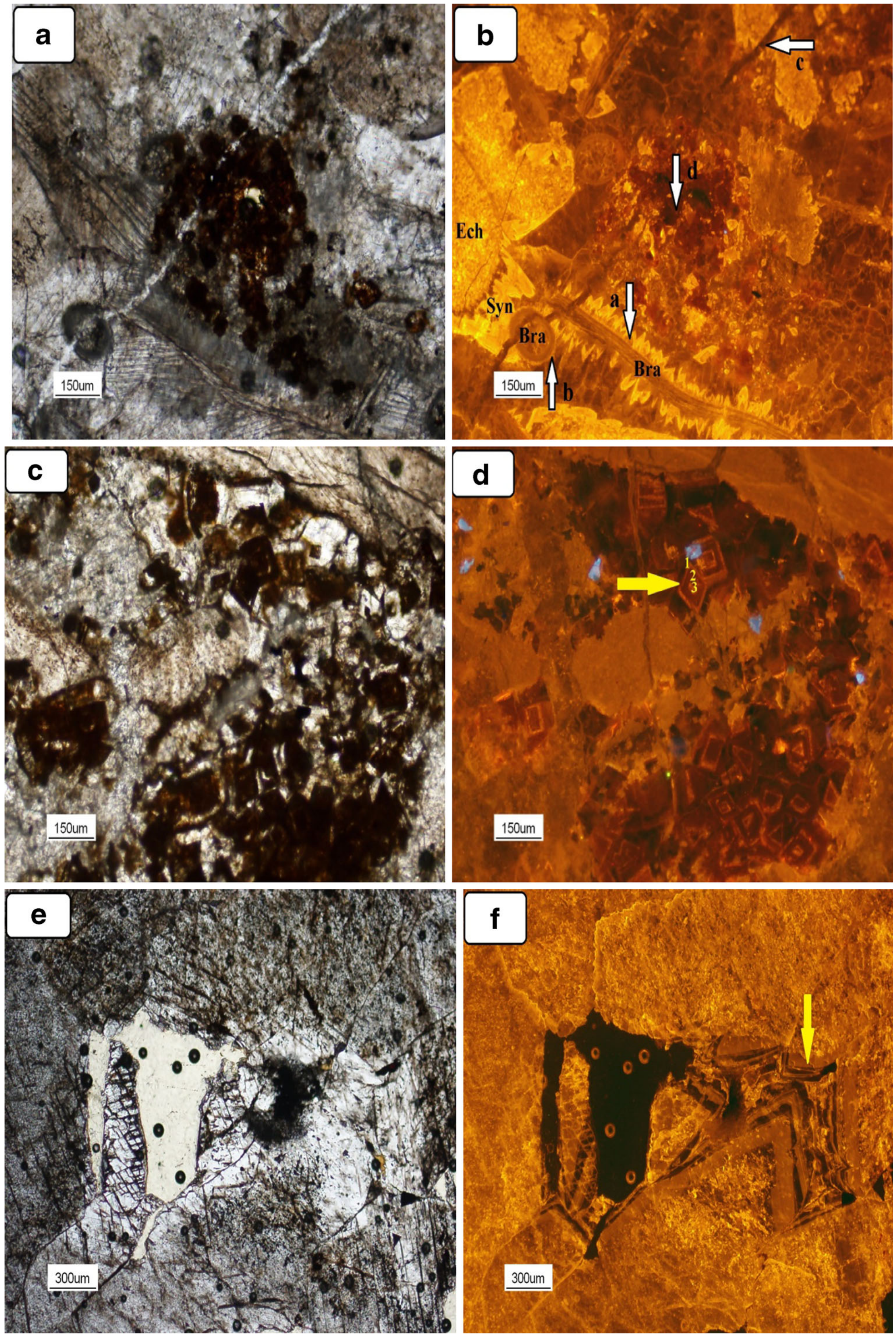

Fig. 10 Diagenetic fabrics and processes studied by Cathodoluminescence in the Bahram Formation Carbonates (**a**) Photomicrograph natural light and cathodoluminescence photograph (**b**) of first generation rim cement which is located around brachiopod by means of partly large (*Arrow a*) and fine (*Arrow b*) crystals. Light luminescence of cement crystals is indicative of high manganese, because Mn has a high concentration in meteoric waters. Dark luminescence is observable from rim toward outside (surface) indicating burial conditions. Syntaxial cement with light luminescence is observable around echinoderm indicating meteoric conditions. Fracturing and filling by calcite cement with dark luminescence (*Arrow c*) is indicative of third generation and formation of dolomite crystals (*Arrow d*) are other diagenetic processes **c** Large and euhedral crystal of dolomite in normal light **d** Cathodoluminescence photograph of previous thin section, yellow arrow is indicative of zonation in dolomite crystal, at least three separate regions are highlighted by numbers 1 to 3 which is indicative of formation in three steps **e** Calcite cement in normal light and **f** Cathodoluminescence photograph of previous thin section, light luminescence and zonation which delineated by yellow arrow, are rather suggestive of meteoric diagenesis origin and change in the liquid chemical component **g** Drusy calcite cement which filled inside the veins, in normal light and **h** Cathodoluminescence photograph of previous thin section, light luminescence is rather suggestive of its meteoric diagenesis origin

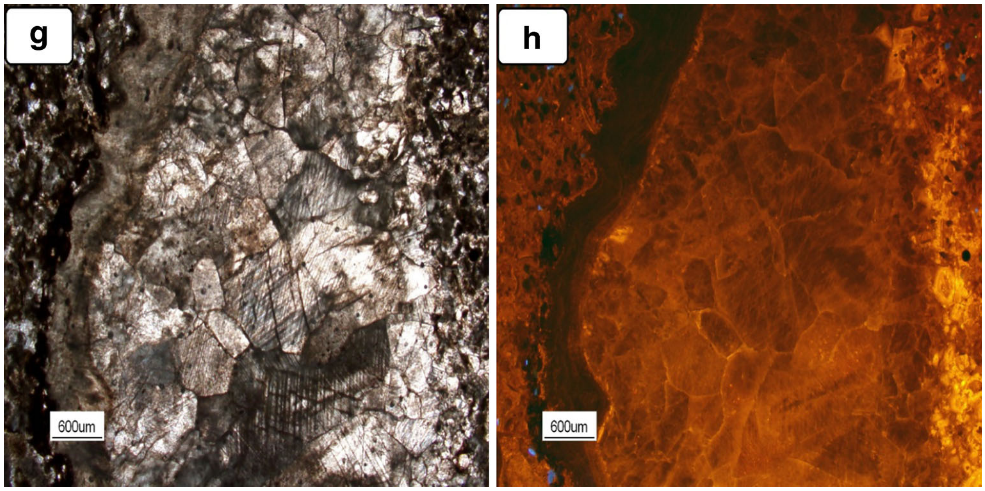

Fig. 10 (continued)

fractures during the final step of diagenesis and uplifting (Flügel 2010). Veins are crossed by stylolite in some of the study samples. Likewise, most of the fractures are filled by Fe-less calcite cement, such phenomenon may be indicative of oxidizing conditions during filling and their formation after uplifting step, fresh water input and weather conditions (Fig. 10a).

Paragenetic sequence

The diagenetic processes in the carbonate limestones took place during different intervals. A region-related paragenetic sequence interpretation is indicative of time of the diagenetic process effects and their succession. On the basis of the petrographic evidence, paragenetic sequence of the Bahram Formation carbonates occurred during four stages as shown in Fig. 9.

- *Marine diagenesis*
  During this stage of diagenesis, some processes such as dissolution on the skeletal grains and formation of secondary porosity, formation of isopachous mosaic and syntaxial overgrowth calcite cements (packstone to grainstone microfacies), and geopetal fabric occurred.
- *Fresh water diagenesis*
  In the Bahram Formation carbonates effects of the marine diagenesis are evidenced by diagenetic fabrics and processes such as isopachous rim cement (high-energy microfacies such as bioclastic grainstone), syntaxial overgrowth cement (packstone to grainstone), bioturbation, micritization (bioclastic wackestone microfacies in lagoon), possibly the presence of fine crystals of dolomite without luminescence and mechanical compaction that affected the carbonates before the main cementation during the early diagenesis (Jadoul and Galli 2008; Ronchi et al. 2011).
- *Burial diagenesis*
  In this diagenesis environment, some process such as grain compaction, drusy, blocky and dog tooth cements, stylolitization, silicification, formation of large crystal of dolomites with white luminescence are indicative of burial conditions.
- Uplift telogenesis
  This stage is characterized by formation of late fractures which crossed stylolites and are filled with hematite cement and pore-filling cement in some thin sections. The absence of luminescence as well as colorless remaining of fracture filling calcite could reflect oxidizing condition during the uplifting (Fig. 10b, Arrow C).

Element geochemical studies

Chemical component of carbonate rocks is a reflection of physical and chemical conditions, incurred during deposition and diagenesis. Therefore, element information patterns may present some information concerning the nature and diagenetic history, effective on the post-depositional carbonates (Adabi 2004; Ronchi et al. 2011). Correct identification of the nature of fluids and diagenesis processes and analysis of carbonate rocks depositional settings is essential for major and minor elements determination and isotopic studies (Mahboubi et al. 2002; Adabi and Asadi-Mehmandosti 2008).

Results of element analysis

Results of element analysis of the Bahram Formation in the study section are presented in Table 1.

Table 1 Major and minor elements changes in the Bahram Formation carbonates in the study regions

Sample No.	Ca (%)	Mg (%)	Fe (ppm)	Mn (ppm)	Sr (ppm)	Na (ppm)
1 (C3)	31.6	0.4	977.6	178.9	289.5	370.9
2 (C15)	32.6	0.3	199.4	271.4	278.5	521.1
3 (C20)	34.1	0.3	88.9	301.7	255.1	485.1
4 (C29)	36.3	0.3	125.5	222.0	405.0	361.6
5 (C37)	39.5	0.4	2238.3	200.5	365.7	722.7
6 (C41)	31.7	0.4	151.9	205.7	447.8	661.2
7 (C45)	35.5	0.3	63.2	292.0	356.9	564.8
8 (C50)	30.3	0.2	159.5	147.3	379.7	532.7
9 (C54)	32.6	0.3	162.4	188.6	348.4	530.8
10 (C55)	33.5	0.3	133.3	187.1	386.3	526.7
11 (C63)	33.9	0.3	138.7	254.3	350.5	642.5
12 (C67)	34.7	0.4	58.7	259.6	298.0	472.1
13 (C68)	38.7	0.4	71.6	172.7	373.8	568.4
14 (C77)	34.8	0.4	58.8	231.4	304.8	559.9
15 (C78)	39.6	0.3	172.0	215.8	428.7	699.6
16 (C92)	39.5	0.6	139.4	957.7	625.0	909.1
17 (K3)	33.4	0.4	21.4	1396.9	278.1	628.6
18 (K4)	30.8	0.3	28.6	2015.0	248.5	599.2
19 (K11)	30.4	0.3	1163.4	1477.3	252.6	508.5
20 (K13)	36.0	0.4	1201.6	1099.9	339.1	754.1
21 (K17)	35.7	0.4	28.6	739.8	356.7	552.2
22 (K19)	35.2	0.4	21.6	802.9	341.6	565.3
23 (K21)	32.1	0.4	32.1	1114.3	427.4	666.3
24 (K24)	29.1	0.4	992.3	761.2	346.5	680.3
25 (K29)	35.6	0.5	32.1	692.0	787.9	677.8
26 (K30)	35.2	0.4	37.0	1051.3	718.0	502.8
27 (K33)	35.1	0.5	436.3	264.5	792.7	618.9
28 (K37)	33.5	0.4	19.1	786.7	846.2	669.5
29 (K44)	38.2	0.3	32.8	1586.8	301.7	426.6
30 (K46)	34.1	0.3	556.6	619.6	655.4	575.0
31 (K51)	38.1	0.3	20.5	1113.2	418.6	465.6
32 (K55)	37.3	0.4	19.8	972.6	416.9	562.7
33 (K63)	39.8	0.5	17.1	1024.7	491.9	630.0
34 (K75)	35.2	0.3	23.7	1436.5	413.4	614.4
35 (D5)	35.1	0.5	229.1	45.5	131.5	403.2
36 (D17)	38.3	0.4	182.1	53.3	121.1	400.3
37 (D18)	30.2	1.1	258.4	58.9	131.4	304.1
38 (D21)	31.7	0.8	185.3	54.3	118.6	367.8
39 (D26)	26.1	1.3	4086.1	405.5	79.5	346.5
40 (D37)	30.1	0.3	4023.4	430.4	332.8	433.2
41 (D40)	29.9	3.4	2401.4	180.9	119.3	335.3
42 (D43)	33.7	3.3	2464.9	176.9	122.5	355.2
43 (D46)	33.6	0.3	653.2	92.7	212.5	321.5
44 (D49)	35.2	0.3	483.3	84.1	185.9	369.5
45 (D640)	39.9	0.4	839.4	114.2	267.7	528.8
46 (D64)	33.2	0.4	1265.4	157.5	138.6	382.3
47 (D65)	35.4	0.6	369.9	64.8	327.6	553.4
48 (D74)	35.1	0.4	355.5	55.5	216.0	480.6
49 (D76)	35.2	0.4	329.3	59.5	202.0	470.8
50 (D78)	35.3	0.3	342.2	83.9	186.7	252.0

Table 1 (continued)

Sample No.	Ca (%)	Mg (%)	Fe (ppm)	Mn (ppm)	Sr (ppm)	Na (ppm)
51 (D81)	39.1	0.3	402.0	85.5	206.3	466.8
52 (D85)	37.2	0.5	924.2	111.0	238.5	485.2

Strontium (Sr)

Assessment of results of element analysis of the Bahram Formation indicates that strontium value in the carbonate deposits of Kamar Kuh section changed from 248.5 to 846.2 ppm (average=476.4 ppm), in Cheshmeh Shir section changed between 255.1 and 625 ppm (average=368.3 ppm) and in Hozedorah changed between 79.5 and 332.8 (average= 187.5 ppm). Strontium value of the samples is low in proportion to recent tropical carbonates which change between 8000 and 10,000 ppm (Milliman 1974) and temperate carbonates which change between 1642 and 5007 ppm (Rao and Adabi 1992; Rao and Amini 1995).

Strontium value is increased with increasing of aragonite content and is reduced with increasing calcite content. Strontium value has low amount in meteoric waters, therefore cause to reduce the strontium value in the carbonates affected by these waters. Strontium abundance in carbonates depends on their mineralogy components, because Sr concentration in the old carbonates reduced considerably during meteoric diagenesis, and is indicative of increasing in calcite mineralogy in relation to aragonite. This reduction may be indicative of meteoric and burial diagenesis (Winefield et al. 1996). There is a relationship between strontium value and rock type (microfacies or lithology) or depositional environments (shallow marine environments versus deep marine environments). Most of the old carbonate rocks omitted their strontium during diagenesis such as aragonite transformation to calite, dissolution and affecting by open system diagenesis (Flügel 2010). Strontium differences of the study samples are due to difference in depositional setting and facies type in three study sections; so that on the basis of facies evidence, extension of the outer ramp facies is reduced toward south of the basin.

Sodium (Na)

Sodium value in recent tropical non-biogenetic aragonite carbonate rocks is variable between 1500 and 2700 ppm (average=2500 ppm). Sodium concentration is up to 270 ppm in the recent temperate non-biogenetic low Mg-calcites (Veizer 1983). Sodium concentration in carbonate deposits is controlled by some factors such as salinity degree, mineralogy, water depth, biogenetic differentiation, and kinetic effects (Adabi and Asadi-Mehmandosti 2008; Rao and Adabi 1992). Sodium value is increased according to salinity, water depth, and aragonite value increasing; and it is low in meteoric waters. Sodium values of the study samples in the Kamar Kuh section are evaluated between 426.6 and 754.1 ppm (average=593.9 ppm), in Cheshmeh Shir section between 361.6 and 909.1 ppm (average=577.8 ppm) and in Hozedorah between 252 and 553.4 (average=403.1 ppm). The low sodium value in the study samples in proportion to recent aragonite can be attributed as another evidence for both calcitic primary mineralogy component of the study samples and effect of meteoric waters.

Manganese (Mn)

Manganese value in the recent aragonitic carbonate rocks is less than 20 ppm and in the recent temperate carbonate samples is more than 300 ppm (Rao and Adabi 1992). Manganese value in the study samples of Kamar Kuh section are variable between 264.5 and 2015 ppm (average=1061.7 ppm), in Cheshmeh Shir section between 147.3 and 957.7 ppm (average=267.9 ppm) and in Hozedorah between 45.5 and 430.4 (average=139.5 ppm). High amount of manganese in proportion to recent tropical and temperate carbonate rocks may be

Table 2 A brief comparision and discussion about geochemical data

Elements/Ratios	Data			Discussion
	Kamar kuh	Cheshme shir	Hozedorah	
Sr (ppm)	476.4	368.3	187.5	North-ward decrease in Sr values indicate shallowing depositional environment
Na (ppm)	593.9	577.8	403.1	North-ward decrease in Na values may suggest both more calcitic primary mineralogy of components and effect of meteoric diagenesis
Mn (ppm)	1061.7	267.9	139.5	High amount of Mn in Kamar kuh section may be due to effect of meteoric diagnesis
Sr/Na	0.78	0.65	0.45	The low Sr/Ca ratio may be considered as a reason for calcitric primary mineralogy. Also, it can be concluded that the paleoclimate conditions at the time of deposition possibbly was similar to recent temperate regions
Sr/Ca	10.53	13.48	5.37	High Sr/Ca ratios show relatively open geochemical system

due to effect of meteoric diagenesis. Manganese value is increased commonly according to meteoric diagenesis processes; because manganese distribution rate is high in meteoric waters (about 15) (Rao 1990; Brand and Veizer 1980). Increasing amount of manganese could be attributed to domination of reduction conditions and also as partially open system. Manganese changes pattern is positive versus strontium, which is due to meteoric diagenesis (Chart 3).

Iron (Fe)

Iron value in the study samples of Kamar Kuh section are variable between 17.1 and 1201.6 ppm (average=295.2 ppm), in Chshmeh Shir section between 58 and 2238.3 ppm (average=308.7 ppm) and in Hozedorah between 182.1 and 4086.1 (average=1203.2 ppm). Iron concentration commonly increases according to increase of insoluble material in acid. As well as iron concentration is increased by water depth reduction, increase of terrigenous entrance and meteoric diagenesis processes and reduction conditions. Under reduction conditions, Fe and Mn are able to join considerably to calcite structure. Effect of meteoric diagenesis is rather confirmed in the study samples because of increase in iron and manganese values and their positive relation with each other and their negative relation with strontium (Charts 1 and 2).

Sr/Na ratio

Sr/Na ratio changes is an important factor to distinguish early mineralogy of aragonite versus calcite and recent and paleotropical carbonates from non-tropical equivalents; so that Sr/Na ratio>1 is indicative of aragonitic early mineralogy and Sr/Na ratio<1 is indicative of calcitic early mineralogy (Winefield et al. 1996; Adabi and Asadi-Mehmandosti 2008).

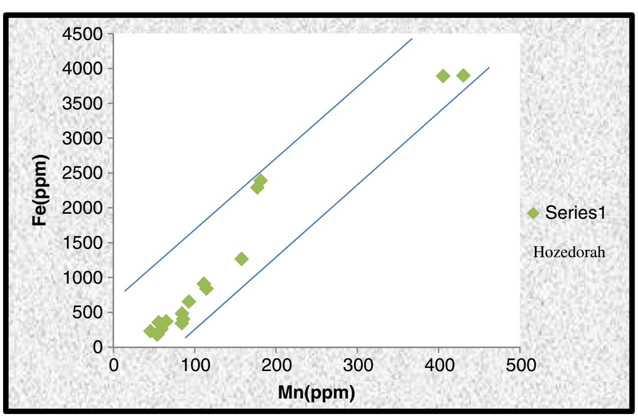

Fig. 11 Plot of Fe values against Mn and Sr. Positive relation of iron and manganese on the basis of closed regression number to 1 and negative relation of iron and strontium are indicative of common origin for both elements during the meteoric diagenesis reduction conditions

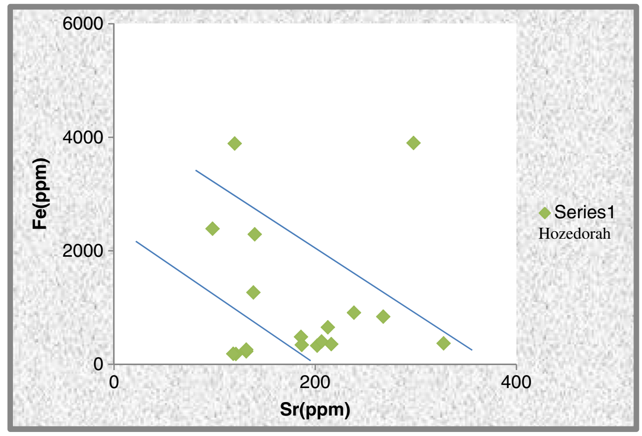

Fig. 12 Plot of Fe values against Mn and Sr. Positive relation of iron and manganese on the basis of closed regression number to 1 and negative relation of iron and strontium are indicative of common origin for both elements during the meteoric diagenesis reduction conditions

Likewise, Sr/Na ratio of recent tropical aragonitic carbonate deposits are between 3 and 5; but this ratio is low (about 1) in recent temperate calcitic carbonate rocks and Mn value is high (Rao 1990). Sr/Na ratio in the study samples of Kamar Kuh section are variable between 0.5 and 1.1 (average=0.78), in Cheshmeh Shir section between 0.5 and 1.1 (average=0.65) and in Hozedorah between 0.2 and 0.8 (average=0.45). Since this ratio in most of the samples is less than 1, therefore it seems that paleoclimate at the time of deposition possibly was similar to recent temperate condition. Investigation of the Middle-Late Devonian geographic maps reveals that the studied region which is located 30^0S had been a part of Gondwana land and geochemical results confirm this fact (Scotese 2014). This low ratio may be considered as a reason for calcitic primary mineralogy of the samples (Chart 5). On the other hand, more reduction of the ratio from Kamar Kuh section (north of basin) toward Hozedorah section (south of basin) shows that Bahram Formation deposits seem to be more calcitic southwards.

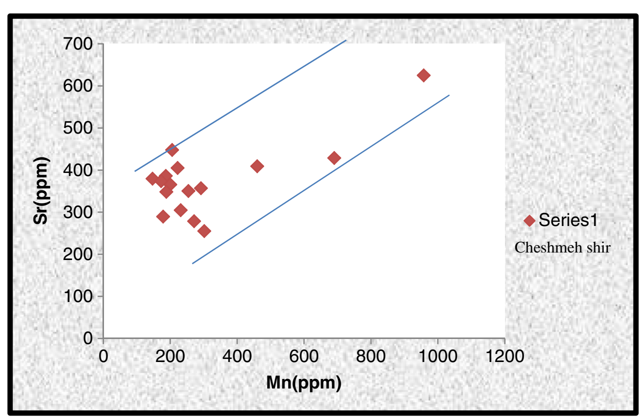

Fig. 13 Pattern changes of Mn against Sr which show a positive pattern, that it is rather due to effect of meteoric diagenesis

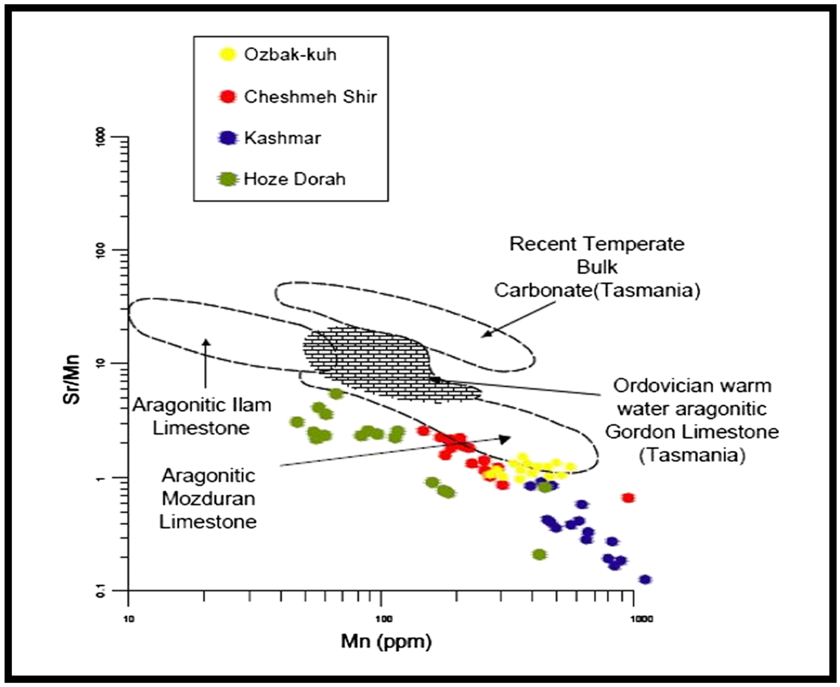

Fig. 14 Changes of Sr/Mn ratio in the study samples of three regions, compared with Ordovician warm water aragonite from the Gordon limestone (Tasmania) (Rao 1990). Aragonite Mozduran limestone (Adabi and Rao 1991). Aragonite Illam limestone (Adabi and Asadi-Mehmandosti 2008), Recent Temperate Bulk carbonate (Tasmania) (Rao and Adabi 1992; Rao and Amini 1995) and samples from Type section of Bahram Formation in Ozbak Kuh (Mahmoudi 2012). Note that all data show low Sr/Mn ratios due to diagenesis in a relatively open environment

Sr/Mn ratio

Bathurst (1975) believes that diagenesis in carbonate rocks is a Wet Dissolution process and Re-precipitation. Therefore, manganse value is increased and strontium value is decreased during dissolution and transformation of semi- stable aragonite to stable calcite.

This process is considerably facilitated by exposure of deposits meteoric fluids (Budd 1992). Since these processes cause the reduction of Sr/Mn ratio, therefore showing the Sr/Mn ratio against Mn may be considered as a criterion for carbonates dissolution (Rao 1991; Adabi and Asadi-Mehmandosti 2008). Sr/Mn ratio in the study samples of Kamar Kuh section are variable between 0.1 and 3, in Cheshmeh Shir section between 0.3 and 2.6 and in Hozedorah between 0.2 and 5.1 and show a reverse pattern with Mn, that is indicative of meteoric diagenesis and dissolution process. In addition, comparison of this ratio and Mn

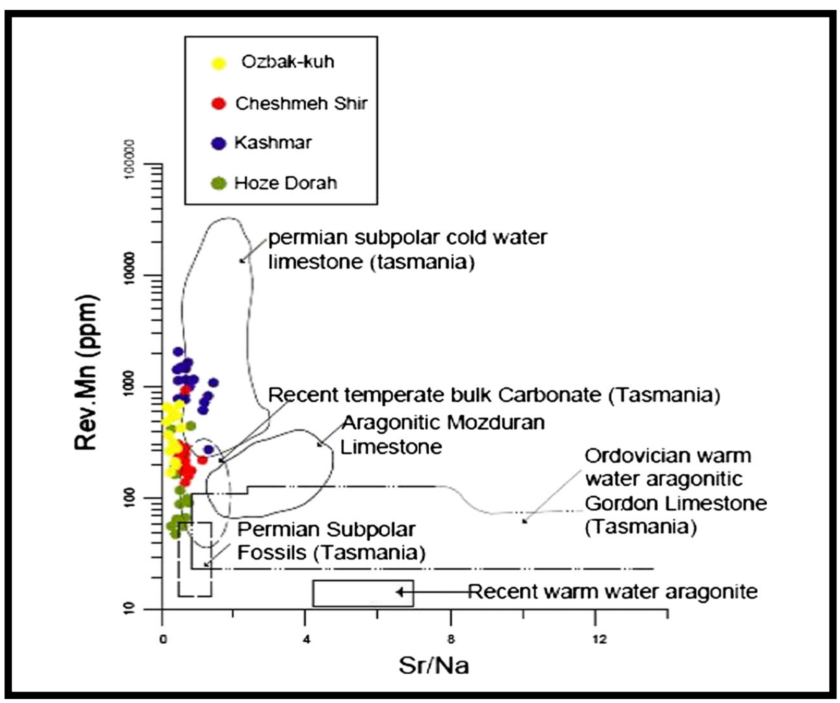

Fig. 15 Changes of Sr/Na ratio against Mn in the study samples of three regions. Note that the Sr/Mn ratios of most samples are <1, indicating the original calcitic mineralogy

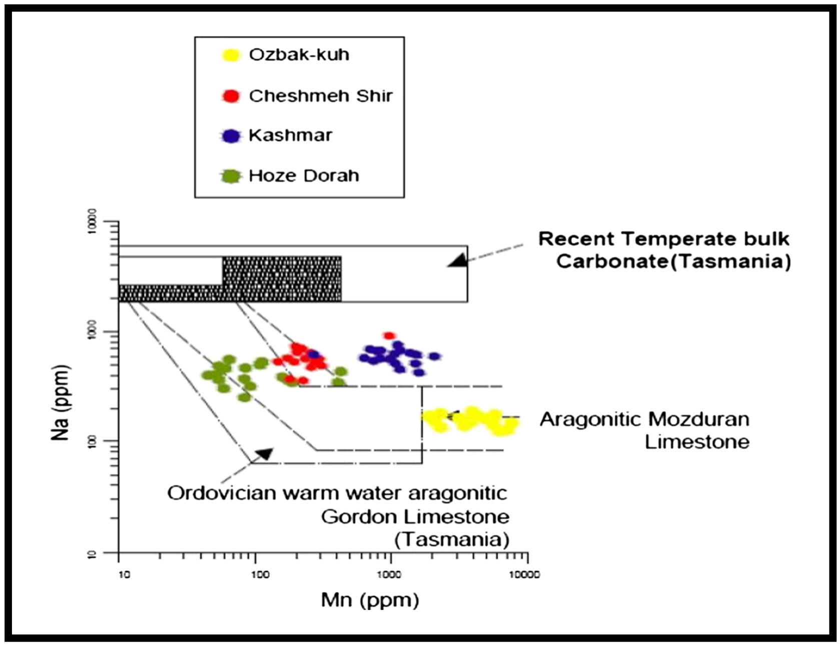

Fig. 16 Changes of Na against Mn in the study samples of three regions

amount in studied region reveals that the meteoric diagenesis has affected the northern part (Kamar Kuh section) more than the southern part (Hozedorah section) (Chart 4).

Sr/Ca ratio

Sr/Ca ratio in carbonates depends on seawater Sr/Ca ratio and strontium distribution factor in carbonates. By means of showing Sr/Ca ratio against Mn, it is possible to determinate diagenesis pattern in closed and open systems. In open diagenetic systems, Sr/Ca ratio is increased due to increase of reaction between water and rock; however, in semi-closed diagenetic systems whose reactions between water and rock are low, this ratio does not have considerable changes on the diagentic phases in proportion to primary component. Increase of Mn content in diagenetic calcite is indicative of open system and effect of reduction waters (Cicera and Lohmann 2001). Sr/Ca ratio in the study samples of Kamar Kuh section are variable between 3.5 and 11.2, in Cheshmeh Shir section between 3.7 and 7.7 and in Hozedorah between 1.4 and 4.9.

A brief comparison of geochemical data is shown Table 2 (Figs. 11, 12, 13, 14, 15, 16).

Conclusion

- Lithographic analysis and investigations together with study of 294 thin sections in three study sections led to recognition of 12 carbonate microfacies and 1 terrigenous facies. Based on microfacies relationship and their distribution, study sections deposited on a carbonate platform (homoclinal ramp type).
- Based on recognized facies groups or assemblages and their distribution patterns in the study sections, the depth of the platform is shallower from north (Kamar Kuh section) toward south (Hozedorah). Besides, barrier facies belt is developed more in Hozedorah section because of the presence of coral boundstone.
- Petrographic evidences show that paragenesis succession of the Bahram Formation carbonates is affected by three steps of diagenesis including eogenesis (marine and meteoric), mesogenesis, and telogenesis. On the basis of low Sr/Mn ratio and Mn amount in studied region reveals that the meteoric diagenesis has affected the northern part (Kamar Kuh section) more than the southern part (Hozedorah section).
- By considering the decrease of Sr and Na values and increase of manganese during the diagenesis and comparison Sr/Na in the study samples with Sr/Na of recent tropical and temperate samples, it seems that the component of the carbonate mud samples of the Bahram Formation, are rather similar to the recent temperate carbonate mud samples. Investigation of the Middle-Late Devonian geographic maps reveals that the studied region which is located 30°S had been a part of Gondwana land and geochemical results confirm this fact.
- Likewise, these changes are also indicative of meteoric diagenesis (including neomorphism) in the study successions.
- The abundance of bioclasts such as echinoid, ostracod and brachiopod together with geochemical evidence such as low strontium content, average of strontium/sodium

ratio, high average of strontium/manganese and low sodium content seem to indicate that the primary mineralogy of carbonates was calcitic.

– Analysis of changing pattern of Sr/Ca ratio against manganese and magnesium show that the diagenetic environments of carbonate rocks were a relatively open environment.

Acknowledgments Department of Geology of Birjand University is much appreciated for providing Laboratory supports. Chemistry Laboratory of Ferdowsi University of Mashhad is also acknowledged for preparing geochemical analysis of major and minor elements. Finally oil Company Research Center and Mr. Mehran Moradpour are thanked for their assistance in taking cathodoluminescence photomicrographs.

References

Adabi MH (1996) Sedimentology and geochemistry of Upper Jurassic (Iran) and Precambrian (Tasmania) carbonates. Unpublished PhD Thesis, University of Tasmania, Australia 470 p

Adabi MH (2004) Sedimentary geochemistry. Arian Zamin, Iran, p 448, **In Persian**

Adabi MH, Asadi-Mehmandosti E (2008) Microfacies and geochemistry of the Ilam Formation in the Tange-E Rashid area, Izeh, S.W., Iran. J Asian Earth Sci 33:267–277

Ahmadzadeh Heravi M, Ashoori A, Gandomi R (2007) Study of brachiopods of the Bahram Formation in Cheshmeh Shir section (Ozbak Kuh, northeast of Tabas). The 7th Annual Symposium of Geological Society of Iran, 6 p

Alavi-Naini M (2009) A brief review on stratigraphy of Iran, Geol Surv. Iran, 507 p

Badenas B, Aurell M (2009) Facies models of a shallow-water carbonate ramp based on distribution of non-skeletal grain (Kimmeridgian, Spain). Facies 56:89–110

Bahari R, Khaksar K, Ashoori A (2006) Investigation of upper Givetian-Frasnian corals of the Bahram formation, South of Ozbak Kuh, Geosciences, 15th year, n 59:56–69

Bathurst R (1975) Carbonates sediments and their diagenesis. Developments in sedimentology, vol 12. Elsevier, Amsterdam, 658 p

Bosence DWJ, Wilson RCL (2003) Carbonate depositional systems. In: Coe A (ed) The sedimentary record of sea-level change. The Open University/Cambridge University Press, Cambridge, 209 p

Brand U, Veizer J (1980) Chemical diagenesis of multicomponent carbonate system, I: trace elements. J Sediment Petrol 50:1219–1236

Brasier AT, Fallick AE, Prave AR, Melezhik AV, Lepland A (2011) Coastal sabkha dolomites and calcitised sulphates preserving the Lomagundi-Jatuli carbon isotope signal. Precambrian Res 189(1–2):193–211

Budd DA (1992) Dissolution of high-Mg calcite fossils and the formation of biomolds during mineralogical stabilization. Carbonates Evaporites 7:74–81

Carols LJ (2002) Diagenetic history of the upper Jurassic Smackover formation and its effect on reservoir properties: Vocation field, Manila Sub-basin, eastern gulf coastal plain. Gulf Coast Assoc Geol Soc Trans 52:631–644

Carozzi AV (1989) Carbonate rock depositional model: a microfacies approach. Prentice-Hall, USA, 604 p

Cicera A, Lohmann KC (2001) Sr/Mg variation during rock-water interaction: implication for secular changes in elemental chemistry of ancient seawater. Geochim Cosmochin Acta 65:741–761

Cook ML, Simo JA, Underwood CA, Rijken P (2006) Mechanical stratigraphic controls on fracture pattern within carbonates and implications for groundwater flow. Sediment Geol 184:225–230

Dickson JAD (1965) A modified staining technique for carbonate in thin section. Nature 205:587

Dunham RJ (1962) Classification of carbonate rocks according to depositional texture. In: Ham, W. E., (eds.), Classification of carbonate rocks. Amer. Assoc. Petrol. Geol. Mem 1:108–121

Eftekharnezhad et al (1972) Geological map of the Kashmar. Geol Surv. Iran;1:250000

Ehrenberg SN, Pickard NAH, Svana TA, Oxtoby NH (2002) Cement geochemistry of photozoan carbonate strata (upper carboniferous-lower Permian), Finnmark carbonate platform, Barents Sea. J Sediment Res 72:95–115

Einsele G (2000) Sedimentary basin, evolution, facies and sediment budget, 2nd edn. Springer, Heidelberg, 292 p

El- Hefnawi MA, Hashaly AO, Shalaby BN, Rashwan MA (2006) Petrography and geochemistry of Eocene limestone from khashm Al- raqaba area: El-calala El-qibliya, Egypt. Carbonates Evaporites 25:193–202

Embry AF, Klovan JE (1972) A late Devonian reef on North Easter Banks Island, North West Territories. Bult Can Petrol Gect 19:730–781

Flügel E (2010) Microfacies analysis of carbonate rocks: analysis, interpretation and application. Springer, Heidelberg, 976 p

Garcia-Pichel F (2006) plausible mechanisms for the boring on carbonates by microbial prototrophs. Sediment Geol 105:29–50

Geel T (2000) Recognition of stratigraphic sequence in carbonate platform and slope deposits, empirical models based on microfacies analysis palaeogene deposits in southeastern Spain. Palaeogeogr 155:211–238

Gregg JM, Shelton KL (1990) Dolomitization and dolomite neomorphism in the back reef facies of the Nonneterre and Davis formation (Cambrian), Southeastern Missouri. J Sediment Petrol 60: 549–562

Haijun ZH, Lin D, Xunlian W, Lei W, Quinshang W, Guoying X (2006) Carbonate diagenesis controlled by glacioeustatic sea-level changes, a case study from the Carboniferous-Permian boundary section at Xikou, China. J China Univ Geosci 17(2):103–114

Heydari E, Wade W (2003) Massive recrystallization of low-Mg calcite at high temperature in hydrocarbon source rocks, Implications for organic acids as factor in diagenesis. AAPG Bull 86:1285–1303

Holcova Z, Zagorsek K (2008) Bryozoa, foraminifera and calcareous nannoplankton as environmental proxies of the bryozoans event in the Middle Miocene of the Central Paratethys(Czech Republic). Paleogeography, Paleoclimatology, Paleoecology 267:216–234

Immenhauser CN, Amour F, Mutti M, Preston R, Fiona F, Whitaker FF, Peterhansel A, Egenhoff SO, Paul A, Dunn PA, Agar SM (2012) Triassic Latemar cycle top sub-aerial exposure of platform carbonates under tropical arid climate. Sediment Geol 265:1–29

Jadoul F, Galli MT (2008) The Hettangian shallow water carbonates after the Triassic Jurassic biocalcification crisis: the Albenza formation in Western Southern Alps. Riv Ital Paleontol Stratigraphy 114:453–470

Johnson AW, Shelton KL, Greeg MJ, Somerville ID, Wright WR, Nagy ZR (2009) Regional studies of dolomites and their included fluids: recognizing multiple chemically distinct fluids during the complex diagenetic history of Lower Carboniferous (Mississipian) rocks of the Irish Zn-Pb ore field. Petrol 96(p):1–18

Kasih GAA, Chiba S, Yamagata Y, Shimizu Y, Haraguchi K (2008) Modelling early diagenesis of sediment in Ago Bay, Japan, a comparison of steady state and dynamic calculations. Ecol Model 215: 40–54

Khalifa MA (2005) Lithofacies, diagenesis and cyclicity of Lower Member of Khuff Formation (Late Permian), Al Qasim Province, Saudi Arabia. J Asian Earth Sci 78:100–123

Lambert L, Durlet C, Loreau JP, Marnier G (2006) Burial dissolution of micrite in Middle East carbonates reservoirs (Jurassic Cretaceous), keys for recognition and timing. Mar Pet Geol 23:79–92

Lasemi Y, Jahani D, Amin-Rasouli H, Lasemi Z (2012) Ancient carbonate tidalites. In: Davis RA, Dalrymple RW (eds) Principle of tidal sedimentology. Springer, Dordrecht, 621 p

Longman MW (1980) Carbonate diagenetic textures from near surface diagenetic environment. AAPG Bull 64:461–487

Mahboubi A, Moussavi-Harami R, Brenner RL, Gonzalez LA (2002) Diagenetic history of late Paleocene potential carbonate reservoir rocks, Kopet Dagh basin, NE Iran. J Pet Geol 25:465–484

Mahmoudi F (2012) Study of peterography and sedimentary environment of the Bahram Formation (Middle-Late Devonian) in Ozbak Kuh region, East of Iran, MSc. Thesis, Birjand University. 138p

Maliva R, Siever R (1988) Pre-Cenozoic nodular cherts, evidence for opal-CT precursors and direct quartz replacement. Am J Sci 288: 799–809

Middleton GV (1973) Johannes Walter's law of correlation of facies. Bull Geol Soc Am 8:979–988

Milliman JD (1974) Marine carbonates part 1: recent sedimentary carbonate. Springer, Berlin, 375 p

Palma R, Lopez-Gomez J, Piethe R (2007) Oxfordian ramp system (La Manga Formation) in the Bardas Blancas area (Mendoza Province) Neuquen Basin. Argentina, facies and depositional sequences. Sediment Geol 195:113–134

Rao CP (1990) Geochemical characteristics of cool-temperate carbonate, Tasmania, Australia. Carbonates Evaporites 5:209–221

Rao CP (1991) Geochemical difference between subtropical (Ordovician) temperate (Recent and Pleistocene) and subpolar (Permian)carbonates, Tasmania, Australia. Carbonates Evaporites 6:83–106

Rao CP, Adabi MH (1992) Carbonate minerals, major and minor elements and oxygen and carbon isotopes and their variation with water depth in cool, temperate carbonates, western Tasmania, Australia. Mar Geol 103:249–272

Rao CP, Amini ZZ (1995) Faunal relationship to grain-size, mineralogy and geochemistry in recent temperate shelf carbonate, Western Tasmania, Australia. Carbonates Evaporites 10:114–123

Reinhold C (1998) Multiple episodes of dolomitization and dolomite recrystallization during shallow burial in Upper Jurassic shelf carbonates: eastern Swabian Alb, southern Germany. Sediment Geol 121:71–95

Ronchi P, Jadoul F, Ceriani A, Giulio AD, Scotti P, Ortenzi A, Massara EP (2011) Multistage dolomitization and distribution of dolomitized bodies in early Jurassic carbonate platform (Southern Alps, Italy). Sedimentology 58:532–565

Ruttner A, Nabavi M, Hadjian J (1968) Geology of the Shirgesht area (Tabas area, East Iran) Geol. Surv. Iran, Rep. n 4;133 p

Saber SG (2012) Depositional framework and sequence stratigraphy of the Cenomanian-Turonian rocks on the western side of the Gulf of Suez, Egypt. Cretac Res 37:300–318

Samankassou E, Tresch J, Strasser A (2005) Origin of peloids in Early Cretaceous deposits. Dorset, South England. Facies 51:264–273

Sanders D (2001) Burrow-mediate carbonate dissolution in rudist biostromes (Aurisina, Italy), implications for taphonomy in tropical, shallow subtidal carbonate environments. Paleogeography, Paleoclimatology, Paleoecology 168:39–74

Sandullia R, Raspinib A (2004) Regional to global correlation of lower cretaceous(Hauterivian-Barremian) shallow-water carbonates of the southern Apennines (Italy) and Dinarides (Montenegro), Southern Tethyan Margin. Sediment Geol 165:117–153

Scotese CR (2014) Paleomap project. http://www.scotese.com

Tamasovych A (2004) Microfacies and depositional environment of upper triassic intra-platform carbonate basin; the fatric unit of west Carpathians (Slovakia). Facies 50:77–105

Teedumae A, Shogenova A, Kalastte T (2006) Dolomitization and sedimentary cyclicity of the Ordovician, Silurian and Devonian rocks in South Estonia. Proc Estonia Acad Sci Geol 55:67–87

Touir J, Soussi M, Troudi H (2009) Polyphased dolomitization of a shoal-rimmed carbonate platform: example from the Middle Turonian Bireno dolomites of central Tunisia. Cretac Res 30(p):785–804

Tucker ME (2001) Sedimentary petrology, 3rd edn. Blackwell, Oxford, 260 p

Tucker M, Wright P (1990) Carbonate sedimentology. Blackwell, Oxford, 482 p

Veizer J (1983) Trace elements and isotopes in sedimentary carbonates. Rev Mineral 11:265–300

Vincent B, Emmanuel L, Houel P, Loreau JP (2007) Geodynamic control on carbonate diagenesis: petrographic and isotopic investigation of the Upper Jurassic formations of the paris Basin (France). Sediment Geol 197(p):267–289

Wilson JL (1975) Carbonate facies in geologic history. Springer, New York, **471 p**

Winefield PR, Nelson CS, Hodder APW (1996) Discriminating temperate carbonates and their diagenetic environments using bulk elemental geochemistry, a reconnaissance study based on New Zealand Cenozoic Limestone. Carbonates Evaporites 11:19–31